

# A Simple Temperature-Based Method to Estimate Heterogeneous Frozen Ground within a Distributed Watershed Model

Michael L. Follum<sup>1,2</sup>, Jeffrey D. Niemann<sup>2</sup>, Julie Parno<sup>3</sup>, and Charles W. Downer<sup>1</sup>

<sup>1</sup>Coastal and Hydraulics Laboratory, Vicksburg, MS, 39180, USA.

<sup>2</sup>Department of Civil Engineering, Colorado State University, Fort Collins, CO, 80523, USA.

<sup>3</sup>Cold Regions Research and Engineering Laboratory, Hanover, NH, 03755, USA.

*Correspondence to:* Michael L. Follum (Michael.L.Follum@usace.army.mil)

## Summary of Author Response

We would like to thank all three Referees for their comments and suggestions. We appreciate all of the insights about the manuscript that have led to several changes that we believe have made this a stronger submission. The response from the authors is broken into four sections followed by the “marked-up manuscript”. The first three sections respond directly to comments made by each Referee, with the last section being a list of References. Each response includes the comments from the Referees, our response to the comment, and the manuscript changes that were made to address the comment. All line and page numbers refer to the “clean” manuscript (with no changes marked). The “marked-up manuscript” begins on Page 14.

## 1 Referee #1

### 1.1 Comments from Referee #1

The aim of this study was to come up with a simple index-based soil frost distribution model for hydrological purpose that can capture spatial variabilities in snow depth and vegetation cover. To this end, the authors extended an old, well-established frost index model (CFGF) and combined it with a modified temperature-index snow model. The snow and soil frost models were tested against data of five winters from an experimental watershed in Vermont. The results show some improvements of the simulated snow and soil frost depths, but they also highlight that simple, index-based models have their limitations in representing the temporal and spatial distribution of snow and soil frost. The distribution of snow and soil frost depth is indeed a complex problem for northern latitude and high-altitude regions of the world – in particular where a vegetation cover is present. Research studies with the objective to improve the simulation of snow and soil frost depth for hydrological purposes have been numerous in the past twenty years : : : not only in north America, but also in Europe. For example, a physically based model (<http://www.coupmodel.com/>) was developed in Sweden some twenty years ago, has been made available (open access) and has been used for snow and soil frost simulations in Nordic and alpine countries, as

well as for sites in Greenland. This model calculates the combined heat and water balance of a soil profile and accounts for interception processes and the presence of a variable snow cover (quite similar to the snow model in this manuscript). So what's the advantage of using a simpler index-based model?

In former times, the main argument was that such index-based models only needed one or few input variables (typically air temperature), whereas physically-based models need five or more meteorological input variables (cf. page 2, lines 11 and 12) and maybe a considerable amount of parameter settings. That's certainly a valid point for many applications. But here in this work, it seems that the new snow and soil frost model is not really simple and index-based, but is going in the direction of a more physically-based approach. Also it apparently needs not only air temperature, but also precipitation, wind speed, relative humidity and cloud coverage. Thus, the argument for developing a new index-based model (instead of using an established physically based model) is not obvious.

The snow and soil frost model modifications proposed in this work are reasonable. Improving a pure air temperature index snow model with a radiation term and accounting for snow interception is certainly of added value for an area such as the Sleepers River experimental watershed where the topography and the vegetation cover is distinctive. And adding a variable soil moisture content and a litter cover to the soil frost model is relevant as these are two important controls of soil frost formation. The core of the new models is a radiation-derived proxy temperature  $T(\text{rad})$  instead of simple air temperature. It would be interesting to see somewhere in this manuscript how much  $T(\text{rad})$  differs from  $T(\text{air})$  in order to clarify whether or not this makes a big difference for the snow model compared to the other modifications. Speaking of  $T(\text{rad})$  I can recommend the following very recent publication (EOS spotlight article <https://eos.org/research-spotlights/how-the-micrometeorology-of-alpine-forests-affects-snowmelt>) for reference: Webster, C., et al. 2017. J. Geophys. Res. Atmos., 122, doi:10.1002/2017JD026581.

The results presented in this manuscript confirm that the modifications made to the original index models are significant and reasonable. Nevertheless, Figures 6 to 8 also clearly show that – even with these more sophisticated models – it is still a long way to reproduce correctly year-to-year variabilities and spatial variabilities in soil frost depth. This is only partially due to the limitations of the model. On the other hand it also reflects the tremendous sensitivity and variability of soil frost in a real landscape. A nice example of such a complex variability in soil frost occurrence was presented in Journal of Hydrology, 546: 90-102, 2017.

The conclusions from this work are plausible, though not really exciting and surprising. And the proposed avenues for further research related to this topic are reasonable. Overall the manuscript is well written and easy to read.

#### Specific comments:

Page 2, line 17: "When the frost index exceeds a threshold, the soil is considered frozen and impermeable to infiltration."

And Page 20, line 7: “: any frozen ground has the potential to impede infiltration and produce flooding” This is not really true. There is a bunch of literature showing that frozen soils are not always impermeable (depending on the ice content), and it needs a certain frost depth for the soil to become impermeable. This could be mentioned somewhere.

Page 8, line 30: “Frost depth was measured using gages described by Ricard et al. (1976) and Shanley and Chalmers (1999).” Please provide some information what principle these measurements are based on. Are these frost tubes containing a blue liquid? Just referring to Ricard and Shanley is not good enough.

Pages 18 and 19: The results in Figures 5 and 6 show very nicely that frost depth is primarily controlled by the snow depth, which in turn is controlled by the forest canopy (or soil management). The air temperature decreasing with altitude is obviously of minor (or no) importance for this elevation range. This is an important message and agrees very well with observations from the lower alps in Switzerland (Journal of Hydrology, 546: 90-102, 2017).

Pages 25 to 29 (References): the cited literature is almost exclusively from North America, but there is a wealth of publications on the observation and spatial modelling of snow and frozen soil from Europe (and other parts of the world) that the authors seem to be unaware of.

The following reference is very relevant to this one and could be mentioned somewhere in the discussion: Campbell, J.L., Ollinger, S.V., Flerchinger, G.N., Wicklein, H., Hayhoe, K., Bailey, A.S., 2010. Past and projected future changes in snowpack and soil frost at the Hubbard Brook Experimental Forest, New Hampshire, USA. Hydrol. Process. 24, 2465–2480, doi: 10.1002/hyp.7666.

## 1.2 Response to Referee #1

Main Issue #1: The frozen ground index method proposed requires numerous forcing data, therefore why use it instead of an energy balance approach?

The main goal of this study is to develop a frozen ground method that improves spatial simulation of frozen ground and can be used within a variety of watershed models in data-sparse environments. This main goal is now more clearly stated in Lines 14-16 on Page 1 and Lines 30-32 on Page 2. We believe that the new modCFGF model has two significant advantages over energy balance approaches within this context. First, many watershed models do not explicitly simulate soil moisture, which would be required to implement an energy balance method (Lines 13-14 on Page 2). The modCFGF method has an option to use soil moisture to simulate the depth of frozen ground, but soil moisture is not required to simulate the presence/absence of frozen ground (Line 10 on Page 3; Lines 18-20 on Page 7; and Line 1 on Page 27). Thus, the modCFGF method can still be used to identify frozen soil for runoff production purposes even when soil moisture is not simulated. Second, the modCFGF method now requires fewer

types of forcing data than many energy balance models, making it more applicable in data sparse regions (Lines 5-7 on Page 28).

The RTI model in the initial manuscript used a common approach for estimating sublimation as described in Liston and Elder (2006), which requires precipitation, temperature, relative humidity, and wind speed data. To reduce the data requirements, a simpler sublimation method based on solar radiation approximations (already calculated in the RTI model) is now used (Lines 3-13 on Page 7). With this revision, the RTI/modCFGI approach requires precipitation, air temperature, and cloud cover forcing data. All of these variables are routinely measured at most airports (data archived in the U.S. at the National Centers for Environmental Information, <https://www.ncdc.noaa.gov/>) as well as many meteorological stations (Line 19 on Page 10 – Line 1 on Page 11; and Lines 9-11 on Page 28). If frost depth is required, then relative humidity, pressure, and wind speed forcing data may still be required to simulate evapotranspiration and soil moisture.

To better address the reviewer's comments, the revised paper now includes a clearer statement of the paper's goals (Lines 14-16 on Page 1; and Lines 30-32 on Page 2), a short discussion of data and parameter requirements in the Model Application section (starting on Line 8 on Page 10), and a discussion of the model's use in data-sparse environments in the Conclusions (Lines 5-13 on Page 28).

Main Issue #2: Results are OK, but not exciting.

We agree that simulating temporal variability of frost depth remains a difficult problem for this model and others. However, the results in this paper are still a valuable contribution for three reasons. First, although index-based models are commonly used in practice, very few studies have tested such models against observed frost depths. This study provides a rare evaluation of the existing CFGI model. Second, the proposed modCFGI model performs much better than the CFGI model in capturing the temporal and spatial variability of frozen ground within the watershed (Figures 6 and 7, Tables 5 and 6). Figure 7 and Table 5 show that the modCFGI model better captures the different frost depths at the various sites in the watershed. Regarding temporal variability, the modCFGI better reproduces the high (e.g., WY 2007) and low (e.g. WY2008) frost depths in Figure 7 and better captures the presence of frozen ground (Table 6). Third, the study shows that much of the spatial variation of frozen ground in the watershed is controlled by insulating ground litter (Lines 18-19 on Page 24; and Conclusion 5 on Page 27). Although ground cover is well known to affect frozen ground, we believe the role of litter cover has not been fully appreciated in previous studies using index-based approaches. The method used to represent litter depth is transferrable to other index-based frozen ground models.

Specific Comment #1: Interesting to see comparison of radiation-derived proxy temperature ( $T_{rad}$ ) to air temperature ( $T_a$ ).

Figure 4 on Page 19 was added to compare  $T_{rad}$  and  $T_a$  at all 8 test plots for a two week period in March 2005. The figure is also used to understand the similarities and differences between the snow simulations at the test plots (Figure 3), specifically related to the role of topography and vegetation on the energy balance (Lines 4-15 on Page 16). Because the plot sites are typically located along shallow slopes where terrain has limited influence, Figure 4 mostly highlights the differences in vegetation. The impact of  $T_{rad}$  on snowpack was also examined in Follum et al. (2015), where four sites at approximately the same elevation but varying in aspect and vegetation type were examined and showed that topography has a dominant role in estimating  $T_{rad}$  and therefore the snowpack. Because  $T_{rad}$  relies on relationships between topography/vegetation and temperature, the work by Webster et al. (2017) was also included as a potential means to improve the estimation of  $T_{rad}$  (Lines 20-22 on Page 28).

Specific Edit Page 2, Line 17: Inaccurate Statement – “When the frost index exceeds a threshold, the soil is considered frozen and impermeable to infiltration.”

We agree that frozen soils are not completely impermeable to infiltration, especially in forested environments (Lindstrom et al. 2002; Bayard et al., 2005; Nyberg et al., 2001; Shanley and Chalmers, 1999). However, this statement is referring to how some hydrologic models use index-based frozen ground methods (such as CFGI) to restrict infiltration. Lines 20-22 on Page 2 were added to clarify that this is often an incorrect assumption.

Specific Edit Page 20, Line 7: Inaccurate Statement – “...because any frozen ground has the potential to impede infiltration and produce flooding.”

This statement was modified to: “...because even shallow frost with high moisture content (concrete frost) has the potential to impede infiltration” (Lines 6-7 on Page 23). A reference to Dunne and Black (1971) is also provided because they observed thin layers of concrete frost increasing the runoff production from plots within SREW.

Specific Edit Page 8, Line 30: Improve description of frost tubes.

The CRREL-Gandahl frost tubes (Ricard et al., 1976) were used at SREW. The reviewer is correct—the frost tubes were filled with a methylene blue solution where freezing depth is identified by a change in color within the tube (blue indicates thawed, clear indicates frozen). A better description of the frost tubes is now given in Lines 18-21 on Page 9. A reference to Vermette and Kanack (2012) is included because they provide images and descriptions of frost tubes that are similar to those used at SREW. A reference to Shanley and Chalmers (1999) is included because they describe the implementation of the frost tubes at SREW.

Specific Edit Reference recent literature in regards to Figure 5 & 6 on Pages 18 and 19:

We agree with the reviewer that the change in elevation (and thus temperature) has small effect on snow and frozen ground within SREW (now shown in greater detail with addition of Figures 4). We appreciate the recommendation

to cite the recent work by Stähli (2017), which is now referenced in Line 30 on Page 1; Lines 4 and 28 on Page 2; and Line 13 on Page 20.

Specific Edit Pages 25-29: Cited literature almost exclusively from North America

5 We agree. Research from outside North America is now better represented in this paper, especially in the first two paragraphs of the Introduction (starting on Line 25 of Page 1). Some of the added references include: Bayard et al. (2005); Bayard and Stähli (2005); Chen et al. (2007); Jansson (2001); Jansson and Karlburg (2010); Lindstrom et al. (2002); Nyberg et al. (2001); and Stähli (2017).

10 Specific Edit Pages 25-29: Include Campbell et al., (2010) as a reference.

The research by Campbell et al. (2010) is now included in the Introduction (Line 30 on Page 1) and Conclusions (Line 24, Page 28) sections.

## 2 Referee #2

### 2.1 Comments from Referee #2

15 The paper by Follum and co-authors seeks to develop a new ‘simple’ temperature based method to estimate frozen ground in a hydrology model. First, the issue of simulating frozen ground is critical for watershed models, particularly in much of the world where frozen ground strongly influences the rate, timing and magnitude of hydrological fluxes. There is a long history of incorporating degree-day and other frozen ground methodologies into hydrological models as the authors state, but of course they are by their nature highly calibrated. The authors state that frozen ground models that are more  
20 physically based (such as SHAW) are highly calibrated and state there is a need for temperature index models that incorporate more physical parameters (i.e. ground cover, radiation derived temperature indices, etc). I have no doubt that this is the case, but in this paper the authors present a highly parametrized and calibrated degree-day model. It works okay, but certainly not great. In fact, I think there is enough forcing data here to drive SHAW and/or other more physically based land-surface schemes with frozen ground. Cloud cover and other radiation parameters are rarely measured operationally, and the  
25 adjustments of the TI portion of the model rely heavily on empirical adjustment. While going down the road of complexity, the authors include some new process representation (interception/unloading), while neglecting sublimation and others. The frozen ground model is adjusted to better improve physical representation, but it does not represent an advancement of our understanding of frozen ground process as the method of simulation is largely empirical and parameters are not transferrable. The strength of simple models is their ease of use and simplicity - but here we have a simple model that gets more and more  
30 complex and requires parameterization that truly limits its applicability and does not justify its use when compared to existing models in the literature. While I can see that developing a local or improved freezing model is important in forecasting and

operations, I do not believe that this paper in advances our understanding of frozen ground processes at a fundamental level that would justify publication in HESS. Perhaps a more operational journal would be the appropriate venue for this work.

## 2.2 Response to Referee #2

Main Issue #1, The frozen ground index method proposed is highly parameterized and requires many forcing data often not measured operationally (cloud cover and other radiation parameters).:

The main goal of this study is to develop a frozen ground method that improves spatial simulation of frozen ground and can be used within a variety of watershed models in data-sparse environments. This main goal is now more clearly stated in Lines 14-16 on Page 1 and Lines 30-32 on Page 2. Although it is difficult to determine the total number of parameters that are required by energy balance models, the modCFGF likely requires specification of many fewer parameters, which reduces the potential for equifinality. The modCFGF method now also requires fewer types of forcing data than many energy balance models, making it more applicable in data sparse regions (Lines 5-7 on Page 28).

The RTI model in the initial manuscript used a common approach for estimating sublimation as described in Liston and Elder (2006), which requires precipitation, temperature, relative humidity, and wind speed data. To reduce the data requirements, a simpler sublimation method based on solar radiation approximations (already calculated in RTI model) is now used (Lines 3-13 on Page 7). With this revision, the RTI/modCFGF approach requires precipitation, air temperature, and cloud cover forcing data. We agree with the reviewer that radiation data are often difficult to obtain operationally. However, operational precipitation, temperature, and cloud cover data are all routinely measured at most airports (data archived in the U.S. at the National Centers for Environmental Information, <https://www.ncdc.noaa.gov/>) as well as many meteorological stations (Line 19 on Page 10 – Line 1 on Page 11; and Lines 9-11 on Page 28). The modCFGF method also has an option to use soil moisture to simulate the depth of frozen ground, but soil moisture is not required to simulate the presence/absence of frozen ground (Line 10 on Page 3; Lines 18-20 on Page 7; and Line 1 on Page 27). Thus, the modCFGF method can still be used to identify frozen soil for runoff production purposes even when soil moisture is not simulated, providing a means to simulate frozen ground in hydrologic models that do not explicitly simulate soil moisture content (Line 14 on Page 2; and Lines 7-9 on Page 28). If soil moisture simulation is needed for frost depth estimation, the inclusion of relative humidity, pressure, and wind speed forcing data may still be required to simulate evapotranspiration and soil moisture.

To better address the reviewer's comments, the revised paper now includes a clearer statement of the paper's goals (Lines 14-16 on Page 1; and Lines 30-32 on Page 2), a short discussion of data and parameter requirements in the

Model Application section (starting on Line 8 on Page 10), and a discussion of the model's use in data-sparse environments in the Conclusions (Lines 5-13 on Page 28).

Main Issue #2, New methods include some improved representation of the snowpack, but not all parts of the snowpack (e.g. sublimation):

The reviewer is correct—neither the TI nor RTI snow models include all processes within the snowpack. The main purpose for using the RTI snow model is to better represent the spatial heterogeneity of the snowpack in data-sparse regions. Specifically, it includes melt from both short- and long-wave radiation through use of  $T_{rad}$ , which Follum et al. (2015) showed improves the spatial simulation of the snowpack by better accounting for topography and vegetation. We agree that some processes such as the movement of snow by wind are neglected by both the TI and RTI models.

Like SNOW-17, both the RTI and TI models can crudely account for interception / sublimation /condensation through a precipitation multiplication factor ( $S_{cf}$ ) (Anderson 2006) typically applied uniformly to the watershed (Lines 28-30 on Page 3; and Lines 3-4 on Page 7). The initial manuscript set  $S_{cf}$  equal to 1, while calculating canopy sublimation in the RTI model using the common approach described in Liston and Elder (2006). The updated manuscript calibrates  $S_{cf}$  in the TI model and in the RTI model uses spatially-varying estimates of sublimation based on solar radiation. The simple method (described in Lines 3-13 on Page 7) estimates sublimation based on the incident solar radiation (and thus land cover and topography). The method neglects wind speed and relative humidity, which affect sublimation rates, but those variables are not available in many cold-region watersheds. Nonetheless, it does vary sublimation rates based on prevalence to solar radiation, which can control sublimation rates and therefore the variability of the snowpack (Gustafson et al., 2010).

Main Issue #3, Modified model improves physical representation, but it does not represent an advancement of our understanding of frozen ground processes and is not transferrable.:

We believe this paper provides three significant advances in our understanding of frozen ground. First, it provides an evaluation of an existing degree day frozen ground model (the CFGI model). Although index-based methods are often used in practice, they have been rarely tested against observations of frost depth. Thus, the results provide useful insights into the performance of this class of models. Second, the new modCFGI model is better suited for use in a wide range of watershed models than other existing frozen ground models. Existing index-based methods poorly reproduce the spatial variations in frozen ground because they do not fully account for the influence of topographic and canopy variations, as shown in this study (Conclusions 3-5 on Pages 27 and 28). Reproducing the spatial pattern of frozen ground is expected to be critical in capturing its role in flood production. The modCFGI model has better performance than the CFGI model in this respect (Figures 6 and 7, and Tables 5 and 6). In



comparison to energy balance models, the modCFGI model requires less forcing data and fewer parameters, and it does not require simulation of soil moisture (which is not explicitly simulated in many watershed models). Thus, we believe the new modCFGI model has significant practical value beyond its use in this study. Third, the study shows that much of the spatial variation of frozen ground in the watershed is controlled by insulating ground litter (Lines 18-19 on Page 24; and Conclusion 5 on Page 27). Although ground cover is well known to affect frozen ground, we believe the role of litter cover has not been fully appreciated in previous studies using index-based approaches. The method used to represent litter depth is transferrable to other index-based frozen ground models.

To better address the reviewer's comments, the revised paper now includes a clearer statement of the paper's goals (Lines 14-16 on Page 1; and Lines 30-32 on Page 2), a short discussion of data and parameter requirements in the Model Application section (starting on Line 8 on Page 10), and a discussion of the model's use in data-sparse environments in the Conclusions (Lines 5-13 on Page 28).

### 3 Referee #3

#### 3.1 Comments from Referee #3

The stated objective of this paper is to better estimate the spatial pattern of frozen ground in a gridded watershed model by modifying a simple cumulative freezing or thawing degree-day approach. This is basically accomplished by (1) using an air temperature index modified by a spatially variable solar radiation index (slope, aspect, elevation) and spatially variable canopy cover to model the snowpack, (2) using shortwave radiation and canopy cover in the calculation of a frost index, (3) using the insulating effects of ground cover when calculating a frost index, and (4), computing frost depth from the frost index by using the "a modified" Berggren Equation. The calculated snow depths and frost depths are then compared to measured snow and frost depths for locations within the Sleepers River Watershed for 5 winters. Snow depths and frost depths were also calculated using the unmodified temperature and frost indices. The results indicate that the modifications implemented generally improved simulations of snow depth, frost depth, and frost occurrence over the 8 spatially diverse sites.

I found that the Introduction to this paper was unnecessarily complicated. Basically, the authors used an air-temperature index modified by a potential solar radiation index (as affected by slope, aspect, and elevation), canopy cover and ground cover. This modified temperature index was then used to drive a snowpack accounting scheme and a frost depth calculation based on cumulative freezing degree-days.

I found the "frozen ground index" and its relationship to the "modified Berggren Equation" unclear. Is the modified Berggren Equation used only after the frozen ground index exceeds a "threshold" value?

Also, equation (16) on page 6 is puzzling to me. There seems to be an  $R_{net}$  term (net all-wave radiation) missing. It should read:  $R_{net} = R_{sw,net} + R_{lw\_down} - R_{lw\_up}$ . Equation (16) makes sense only if  $R_{net}$  is assumed to be zero but that is not stated.

It is unclear from the text if sublimation from the snowpack is accounted for when there is no canopy cover. It appears that sublimation is only calculated from intercepted snow.

Page 13, table 3: The term “residual saturation” is ambiguous, particularly at the low value of 0.038. Is this referring to some “degree of saturation”, ie, some volumetric soil moisture expressed as a fraction of the saturated volumetric moisture content?

Page 23, line 4. Should read “requires more energy loss to cool and freeze the soil”

Overall, the authors are to be commended for their sound modeling procedures that included several field test sites, distinct calibration versus validation time periods, the sophisticated parameter estimation techniques, and sensitivity analysis. By using a 30-meter grid for capturing spatial variability they were able to generate informative maps of snow depth, frost depth, and snow water equivalent. The use of RMSE and NSE values for each case, as well as plots of absolute simulated and observed values for each time period, were appreciated. The absolute errors were hard to perceive for some data sets simply because of the small size of the graphs. It does appear from the plots that there were cases with high absolute differences between simulated and observed.

I agree with the authors assessment of the model’s strengths and weaknesses, and the need for improved representation of the effects of wind and soil moisture in achieving better accuracy.

### 3.2 Response to Referee #3

Main Issue #1, Introduction unnecessarily complicated:

We have revised the introduction to follow a more logical progression. The first paragraph (beginning on Page 1) states that frozen ground is important in estimating stormflow and highlights the heterogeneity of frozen ground and the causes of the spatial variability. The second paragraph describes the current numerical approaches for simulating frozen ground, with energy balance methods often being too complex to use in many watershed modelling scenarios and index-based approaches often not capturing spatial variability outside of elevation. The third and fourth paragraphs focus on the objective of the study, which is to better estimate the spatial pattern of frozen ground in data-sparse watersheds by modifying a commonly-used index-based approach (Lines 30-32 on Page 2).

Main Issue #2, Relationship between frozen ground index and modified Berggren Equation is unclear.:

The modified Berggren Equation (as shown in Equation 19) is used to estimate frost depth from the frozen ground index  $F$ . The ground freezes when  $F$  reaches a threshold  $F_{threshold}$ , and frost depth increases as  $F$  becomes larger than  $F_{threshold}$ . As  $F$  decreases (due to increased temperatures), the frost depth also decreases until no frost is left

when  $F$  fall below  $F_{threshold}$ . We revised Lines 12-16 on Page 8 to better describe the connection between  $F$  values calculated by CFGI / modCFGI and the modified Berggren Equation.

Main Issue #3, Net radiation term is missing from Equation 16.:

5 Equation 11 (formerly Equation 16) represents a step in obtaining the radiation-derived proxy temperature ( $T_{rad}$ ) for simulation of the snowpack.  $T_{rad}$  is calculated under the assumption that the outgoing long-wave radiation balances the net incoming short-wave and long-wave radiation (Follum et al., 2015). This balance is clearly an approximation, but the implied proxy temperature better represents the available energy than the air temperature. Follum et al. (2015) showed that the use of  $T_{rad}$  can provide a significant improvement in the simulation of  
10 snowpack in a temperature index approach. This assumption is now stated directly in Line 30 on Page 5 – Line 6 on Page 6.

Main Issue #4, Unclear on the inclusion of sublimation of the snowpack.:

15 Like SNOW-17, both the RTI and TI models can crudely account for interception / sublimation /condensation through a precipitation multiplication factor ( $S_{cf}$ ) (Anderson 2006) typically applied uniformly to the watershed (Lines 28-30 on Page 3; and Lines 3-4 on Page 7). The initial manuscript set  $S_{cf}$  equal to 1, while calculating canopy sublimation in the RTI model using the common approach described in Liston and Elder (2006). The updated manuscript calibrates  $S_{cf}$  in the TI model and in the RTI model uses spatially-varying estimates of  
20 sublimation based on solar radiation. The simple method (described in Lines 3-13 on Page 7) estimates sublimation based on the incident solar radiation (and thus land cover and topography). The method neglects wind speed and relative humidity, which affect sublimation rates, but those variables are not available in many cold-region watersheds. Nonetheless, it does vary sublimation rates based on prevalence to solar radiation, which can control sublimation rates and therefore the variability of the snowpack (Gustafson et al., 2010).

25 Main Issue #5, Ambiguous “residual saturation” term.:

The term “residual saturation” was replaced with “residual water content” in Table 3 on Page 14 and in Lines 9-10 on Page 25.

Minor Comment #1, Change in Line 4 of Page 23:

30 We appreciate the correction and changed the text from “require more energy to cool and freeze the soil” to “require more energy loss to cool and freeze the soil” in Line 4 on Page 26.

#### 4 References

Anderson, E.A.: Snow Accumulation and Ablation Model - SNOW-17, NWSRFS User Documentation, U.S. National Weather Service, Silver Springs, MD, 2006.

- 5 Bayard, D., Stähli, M.: Effects of frozen soil on the groundwater recharge in Alpine areas, *Climate and hydrology in mountain areas*. Wiley, Chichester, 73-83, 2005.

Bayard, D., Stähli, M., Parriaux, A., Flühler, H.: The influence of seasonally frozen soil on the snowmelt runoff at two Alpine sites in southern Switzerland, *Journal of Hydrology* 309(1), 66-84, 2005.

10

Campbell, J.L., Ollinger, S.V., Flerchinger, G.N., Wicklein, H., Hayhoe, K., Bailey, A.S.: Past and projected future changes in snowpack and soil frost at the Hubbard Brook Experiment Forest, New Hampshire, USA, *Hydrological Processes*, 24, 2465-2480, 2010.

- 15 Chen, R.S., Kang, E.S., Ji, X.B., Yang, Y., Zhang, Z.H., Qing, W.W., Bai, S.Y., Wang, L.D., Kong, Q.Z., Lei, Y.H., Pei, Z.X.: Preliminary study of the hydrological processes in the alpine meadow and permafrost regions at the headwaters of Heihe River, *Journal of Glaciology and Geocryology*, 29(3), 387-396, 2007.

Dunne, T., Black, R.D.: Runoff processes during snowmelt, *Water Resources Research*, 7(5), 1160-1172, 1971.

20

Follum, M.L., Downer, C.W., Niemann, J.D., Roylance, S.M., Vuyovich, C.M.: A radiation-derived temperature-index snow routine for the GSSHA hydrologic model, *Journal of Hydrology*, 529, Part 3, 723-736, 2015.

- 25 Gustafson, J.R., Brooks, P.D., Molotch, N.P., Veatch, W.C.: Estimating snow sublimation using natural chemical and isotropic tracers across a gradient of solar radiation, *Water Resources Research*, 46(12), 1-14, 2010.

Jansson, P.E.: Coupled heat and mass transfer model for soil-plant-atmosphere systems. 2001.

- Jansson, P.E., Karlberg, L.: Coupled heat and mass transfer model for soil-plant-atmosphere systems, *Royal Institute of Technology*, Stockholm, p. 454, 2010.

30

Lindstrom, G., Bishop, K., Lofvenius, M.O.: Soil frost and runoff at Svartberget, northern Sweden—Measurements and model analysis, *Hydrological Processes*, 16, 3379–3392, 2002.

Liston, G.E., Elder, K.: A distributed snow-evolution modeling system (SnowModel), *Journal of Hydrometeorology*, 7(6), 1259-1276, 2006.

5 Nyberg, L., Stähli, M., Mellander, P.E., Bishop, K.: Soil frost effects on soil water and runoff dynamics along a boreal forest transact: 1. Field investigations, *Hydrological Processes*, 15, 909 – 926, 2001.

Ricard, J.A., Tobiasson, W., Greatorex, A.: The field assembled frost gage, United States Army Cold Regions Research and Engineering Laboratory, Hanover, New Hampshire, 1976.

10 Shanley, J.B., Chalmers, A.: The effect of frozen soil on snowmelt runoff at Sleepers River, Vermont, *Hydrological Processes*, 13, 1843-1857, 1999.

Stähli, M.: Hydrological significance of soil frost for pre-alpine areas, *Journal of Hydrology*, 546, 90-102, 2017.

15 Vermette, S., Kanack, J.: Modeling frost line soil penetration using freezing degree-day rates, day length, and sun angle, 69<sup>th</sup> Eastern Snow Conference, Frost Valley YMCA, Claryville, New York, USA, 2012.

Webster, C., Rutter, N., Jonas, T.: Improving representation of canopy temperatures for modeling subcanopy incoming longwave radiation to the snow surface, *Journal of Geophysical Research: Atmospheres* 122(17), 9154-9172, 2017.

20

25

30

# A Simple Temperature-Based Method to Estimate Heterogeneous Frozen Ground within a Distributed Watershed Model

Michael L. Follum<sup>1,2</sup>, Jeffrey D. Niemann<sup>2</sup>, Julie Parno<sup>3</sup>, and Charles W. Downer<sup>1</sup>

<sup>1</sup>Coastal and Hydraulics Laboratory, Vicksburg, MS, 39180, USA.

<sup>2</sup>Department of Civil Engineering, Colorado State University, Fort Collins, CO, 80523, USA.

<sup>3</sup>Cold Regions Research and Engineering Laboratory, Hanover, NH, 03755, USA.

Correspondence to: Michael L. Follum (Michael.L.Follum@usace.army.mil)

## Abstract

Frozen ground can be important to flood production and is often heterogeneous within a watershed due to spatial variations in the available energy, insulation by snowpack and ground cover, and the thermal and moisture properties of the soil. The widely-used Continuous Frozen Ground Index (CFGF) model is a degree-day approach and identifies frozen ground using a simple frost index, which varies mainly with elevation through a temperature-elevation relationship. Similarly, snow depth and its insulating effect are also estimated based on elevation. The objective of this ~~workpaper~~ is to ~~more accurately represent~~ develop a model for frozen ground that (1) captures the spatial ~~heterogeneity~~ variations of frozen ground within a watershed, (2) allows the frozen ground model to be incorporated into a variety of watershed models, and (3) allows application in a distributed hydrologic model data sparse environments. To do this, we modify the existing CFGF method within the Gridded Surface Subsurface Hydrologic Analysis (GSSHA), by modifying the CFGF method watershed model. Among the modifications, the snowpack and frost indices are simulated by replacing air temperature (a surrogate for the available energy) with a radiation-derived temperature that aims to better represent spatial variations in available energy. Ground cover is also included as an additional insulator of the soil. Furthermore, the modified Berggren Equation, which accounts for soil thermal conductivity and soil moisture, is used to convert the frost index into frost depth. The modified CFGF model is tested by application at six test sites within the Sleepers River Experimental Watershed in Vermont. Compared to the CFGF model, the modified CFGF model more accurately captures the variations in frozen ground between the sites, inter-annual variations in frozen ground depths at a given site, and the occurrence of frozen ground.

## 1 Introduction

Frozen ground (also known as frozen soil or soil frost) can play a significant role in the hydrologic response of watersheds because it impedes the infiltration of snowmelt and rainfall and enhances runoff. For example, Dunne and Black (1971) examined the Sleepers River Experimental Watershed (SREW) in northeastern Vermont and observed that almost 50% of meltwater left research plots as runoff due to frozen ground. Frozen ground has also been shown to contribute to the periodic flooding of the Red River in North Dakota (Stoner et al., 1993), the 1936 floods in New England (Diebold, 1938),

Formatted: Condensed by 0.1 pt

Formatted: Condensed by 0.1 pt

Formatted: Condensed by 0.1 pt

Formatted: Condensed by 0.1 pt

Formatted: Condensed by 0.1 pt

and severe flooding and erosion events in the Pacific Northwest (Johnson and McArthur, 1973). Although the timing and spatial pattern of frozen ground can greatly affect the amount and type of runoff within a watershed (Wilcox et al., 1997), they are often difficult to simulate in many hydrologic models.

is important to predicting stormflows produced by certain watersheds (Shanley and Chalmers, 1999; McNamara et al., 1997; Prêvost et al., 1990; Woo, 1986). Several plot-scale studies have shown that frozen ground can impede infiltration and thus enhance runoff (Bayard et al., 2005; Dunne and Black, 1971; Stähli et al., 1999). Several of these studies have also shown that frozen ground is highly-variable temporally and spatially (Campbell et al., 2010; Shanley and Chalmers, 1999; Stähli, 2017), which affects the amount and type of runoff (Wilcox et al., 1997). The presence, spatial pattern, and depth of frozen ground are driven by mass (water) and energy balances. The energy available from the atmosphere to freeze or thaw the soil is subject to the insulation of the snowpack (Pearson, 1920; Willis et al., 1961) and ground cover including any vegetation, woody debris, and leaf litter (Brown, 1966; Diebold, 1938; Fahey and Lang, 1975; Sartz, 1973; Stähli, 2017). MacKinney (1929) found that ground cover reduced the depth of frost penetration by 40% at a test site in Connecticut. Additionally, the presence and depth of frozen ground is affected by soil moisture (Fox, 1992; Willis et al., 1961) and the thermal conductivity of the soil (Farouki, 1981; Johansen, 1977).

Frozen ground has proven difficult to simulate within distributed hydrologic models due to complex interactions of energy and water between the atmosphere, snowpack, and soil (Dun et al., 2010; Kennedy and Sharratt, 1998; Lin and McCool, 2006). Physically-based models of frozen ground, such as the Simultaneous Heat and Water (SHAW) model (Flerchinger and Saxton, 1989), the coupled heat and mass transfer model for soil-plant-atmosphere systems (COUP) (Jansson 2001; Jansson and Karlburg, 2010), and the Distributed Water-Heat Coupled (DWHC) model (Chen et al., 2007) have large parameter and forcing data requirements—such as wind speed, relative humidity, and short- and long-wave radiation—which restricts their applicability in many watershed. Additionally, these types of models either include, or are tightly coupled to soil moisture models, which can limit their applicability in models that do not explicitly simulate soil moisture content. To reduce the data and parameter requirements and increase applicability, simple temperature-index or degree-day methods have been developed (Molnau and Bissell, 1983; Rekolainen and Posch, 1993) and remain widely used within watershed models, including LISFLOOD (De Roo et al., 2001; Van Der Knijff et al., 2010), CREAMS (Rekolainen and Posch, 1993), and the Gridded Surface Subsurface Hydrologic Analysis (GSSHA) model (Downer and Ogden, 2004). Degree-day approaches typically accumulate the daily average temperature as a frost index (°C-days). When the frost index exceeds a threshold, the soil is considered frozen and impermeable to infiltration. Some The sudden restriction on infiltration can be an incorrect assumption, especially in forested environments where frozen soils often still experience infiltration (Lindstrom et al. 2002; Nyberg et al., 2001; Shanley and Chalmers, 1999). A limitation of degree-day approaches, such as is that they are often untested against observed frost data because the Continuous Frozen Ground Index (CFGDI) (Molnau and Bissell, 1983), account for the insulating characteristics of the snowpack, but these approaches generally do not consider ground cover. Most a physical property that can be compared to measurements. However, degree-day models determine the spatial pattern of frozen ground using a temperature gage, the watershed

elevations, and a lapse rate (which is also used to simulate spatial variations in snowpack that in turn impacts frost depth). Degree-day methods have been successful in capturing increased runoff from frozen ground events ~~that lead to increased runoff~~ (Molnau and Bissell, 1983), and higher frost index values have been shown to correlate to deeper frost depths (Vermette and Christopher, 2008; Vermette and Kanack, 2012). ~~However, testing of degree-day approaches has been limited because the frost index is not a physical property that can be compared to measurements.~~ Spatial variations of frozen ground within degree-day methods are typically based on variations in temperature (which are estimated from an elevation-temperature relationship) and variations in snowpack insulation (which are also typically inferred from an elevation-temperature relationship). Such reliance on elevation may lead to errors because Stähli (2017) found no clear connection between elevation and presence of frozen ground at test sites in the Swiss pre-alpine zone.

The objective of this paper is to ~~better estimate~~ develop a model for frozen ground that (1) captures the spatial ~~pattern~~ variations of frozen ground within a watershed, (2) allows the frozen ground model to be incorporated into a variety of watershed models, and (3) allows application in data sparse environments where limited forcing data may prohibit use of energy balance methods. In this paper, we use the GSSHA watershed model and develop the frozen ground model by modifying the commonly used Conceptual Frozen Ground Index (CFGF) (Molnau and Bissell, 1983) method in four ways. First, the CFGF method is coupled to an improved snowpack model that more accurately captures the spatial heterogeneity of the snowpack. In past applications of GSSHA, the CFGF method has been coupled with a temperature-index (TI) snowpack model based on SNOW-17 (Anderson, 1973; Anderson, 2006). However, Follum et al. (2015) proposed a Radiation-derived Temperature Index (RTI) snow model that uses a proxy temperature instead of air temperature to represent the energy available to the snowpack. Compared to the TI model, the RTI model more directly includes the effects of shortwave radiation and canopy cover and was shown to better represent the spatial variations of snow cover and snow water equivalent (SWE) in the Senator Beck Basin in Colorado. The RTI model is adopted to simulate the snowpack in the present study. Second, the effects of shortwave radiation and canopy cover are included in the CFGF model when calculating the energy available at the snow or ground surface. These effects are included by using a similar radiation-derived proxy temperature when calculating the frost index. Third, the insulation effects of ground cover are included by modifying the frost index equation. Fourth, an option is included to compute frost depth ~~is computed from as a function of~~ the frost index value ~~and is a model output.~~ The modified Berggren Equation and similar Stefan Equation have been previously used to ~~correlate degree-days to estimate~~ frost depth from degree-days (Carey and Woo, 2005; DeWalle and Rango, 2008; Fox, 1992; Woo et al., 2004); a similar approach is used here to convert the frost index to frost depth.

The following sections first describe the existing TI and CFGF models within GSSHA. The combination of these two models serves as the baseline or control case for the experiments. Then, the RTI snow model and the modified CFGF frozen ground model (referred to as modCFGF) are described. Finally, the results of the TI/CFGF model and RTI/modCFGF models are compared to each other and to observations of snow depth, SWE, and frost depth at the SREWSleepers River Experimental Watershed (SREW) in Vermont.



## 2 Methodology

### 2.1 TI Snowpack Model

The TI snow model was implemented into GSSHA by Follum et al. (2014), who provides additional information about the model. Although GSSHA allows a variable time step for multiple processes, it always uses an hourly time step ( $\Delta t$ ) for snow calculations. GSSHA utilizes a structured grid in which each cell can have a different air temperature  $T_a$  ( $^{\circ}\text{C}$ ) and precipitation  $P$  ( $\text{m h}^{-1}$ ). Air temperature is the primary driver of snowpack dynamics in the TI model and is estimated as:

$$T_a = T_g + \emptyset(E_g - E_c), \quad (1)$$

where  $T_g$  ( $^{\circ}\text{C}$ ) is the air temperature at a gage,  $\emptyset$  is a linear lapse rate ( $^{\circ}\text{C km}^{-1}$ ), and  $E_g$  and  $E_c$  (m) are the elevations of the temperature gage and the grid cell where  $T_a$  is being calculated, respectively. Precipitation accumulates as SWE (m) when

$T_a \leq T_{px}$ , where  $T_{px}$  is the freezing point ( $0^{\circ}\text{C}$  by default). ~~Interception of snow by vegetation and the subsequent sublimation, melt, and fall-off are neglected in the TI model.~~ The precipitation  $P$  is multiplied by a uniform multiplication factor ( $S_{cf}$ ), which crudely represents snowpack sublimation and redistribution of snow due to wind (Anderson, 2006). The resultant effective precipitation ( $P_{eff}$ ) is added to the SWE.

Formatted: Not Expanded by / Condensed

Before the snowpack begins to melt, its heat deficit (or cold content) must be overcome. The change in heat deficit

$\Delta D_t$  (mm of SWE), due to a temperature difference between the snow surface and air, is calculated as:

$$\Delta D_t = N_{mf,max}(dt/6)(M_f/M_{f,max})(A_{TI} - T_{sur}), \quad (2)$$

~~where~~ where  $T_{sur}$  is the snow surface temperature, and  $A_{TI}$  is the antecedent temperature index ( $^{\circ}\text{C}$ ), which is calculated using  $T_a$  and the antecedent snow temperature index parameter  $A_{TIM}$ , ~~and  $T_{sur}$  is the snow surface temperature~~ (see Anderson (2006) for details regarding  $T_{sur}$  and  $A_{TI}$  and  $T_{sur}$ ).  $N_{mf,max}$  is the maximum negative melt factor ( $\text{mm } ^{\circ}\text{C}^{-1} (6 \text{ h})^{-1}$ ), which is a parameter.  $M_f$  is the melt factor ( $\text{mm } ^{\circ}\text{C}^{-1} dt^{-1}$ ), which is calculated as:

$$M_f = (dt/6)[S_v A_v (M_{f,max} - M_{f,min}) + M_{f,min}], \quad (3)$$

where  $S_v$  and  $A_v$  are seasonal melt adjustments that change by Julian day, and  $M_{f,max}$  and  $M_{f,min}$  are the maximum and minimum melt factors ( $\text{mm } ^{\circ}\text{C}^{-1} (6 \text{ h})^{-1}$ ), which are parameters.

Once the heat deficit is overcome, SWE decreases as melt occurs. During normal conditions, the melt  $M$  (mm of

SWE) is:

$$M = [M_f(T_a - T_{mbase}) + 0.0125 P_{eff} f_r T_r] \Delta t - [M_f(T_a - T_{mbase}) + 0.0125 P_{eff} f_r T_r] \Delta t, \quad (4)$$

where  $T_{mbase}$  is the temperature at which melt begins ( $0^{\circ}\text{C}$  by default),  $f_r$  is the fraction of any precipitation that is rain (see Anderson (2006) for details assumed equal to 1 when  $T_a > 0^{\circ}\text{C}$ , otherwise set to 0), and  $T_r$  is the precipitation temperature (assumed equal to  $T_a$  or  $0^{\circ}\text{C}$ , whichever is greater). During rain-on-snow events (more than 1.5 mm of rainfall in the previous 6 h),  $M$  is calculated from a simple energy balance:

$$M = \sigma [(T_a + 273)^4 - 273^4] \Delta t + 0.0125 P_{eff} f_r T_r + 8.5 f_u (\Delta t / 6) [(r_h e_{sat} - 6.11) + 0.00057 P_a T_a], \quad (5)$$

where  $\sigma$  is the Stefan-Boltzmann constant,  $f_u$  is the average wind function ( $\text{mm mb}^{-1} (6 \text{ h})^{-1}$ ) (see Anderson (2006) for details),  $r_h$  is the relative humidity (assumed to be 0.9 during rain-on-snow events) (Anderson, 1973, 2006),  $P_a$  is atmospheric pressure (mb) (either measured or calculated from elevation) (Anderson, 2006), and  $e_{sat}$  is the saturation vapor pressure (mb) (calculated based on Smith (1993)). The ripeness of the snowpack affects the amount of melt that is released and is controlled by the liquid holding capacity  $L_{hc}$ , which is a specified percentage of the ice in the snowpack (Anderson, 2006).

For frozen ground calculations, the snow depth is needed from the snow model. The snow depth  $D_s$  (cm) is found from the SWE and the snowpack density. GSSHA uses the single-layer snow density functions from SNOW-17 (Anderson, 1976; Anderson, 2006). The density of newly fallen snow  $\rho_n$  ( $\text{gm cm}^{-3}$ ) varies between 0.05 ( $T_a \leq -15^\circ\text{C}$ ) and 0.15 ( $T_a = 0^\circ\text{C}$ ) according to:

$$\rho_n = 0.05 + 0.0017 (T_a + 15)^{1.5}. \quad (6)$$

Increases in snowpack density  $\rho_x$  from compaction, destructive metamorphism, and melt metamorphism due to the presence of liquid water are calculated as (Koren et al., 1999):

$$\rho_{x,t} = \rho_{x,t-1} \left( \frac{e^{B_2}}{B_2} \right) e^{B_1}, \quad (7)$$

where:

$$B_1 = c_3 c_5 dt e^{c_4 T_s - c_x \beta (\rho_{x,t-1} - \rho_d)}, \text{ and} \quad (8)$$

$$B_2 = W_{t-1} c_1 dt e^{0.08 T_s - c_2 \rho_{x,t-1}}. \quad (9)$$

The variable  $t$  is an index for time,  $W$  is the ice portion of the snow pack (cm,  $W = 100 S_{swe,t-1}$ ) where  $S_{swe}$  is the snow water equivalent on the ground in m,  $T_s$  is the average snow pack temperature ( $^\circ\text{C}$ , calculated based on Anderson (2006)), and  $\rho_d$  is the threshold density above which destructive metamorphism decreases ( $\rho_d$  is set to  $0.15 \text{ gm cm}^{-3}$  based on Anderson (2006)). Finally,  $\beta = 0$  if  $\rho_{x,t-1} \leq \rho_d$ , and  $\beta = 1$  if  $\rho_{x,t-1} > \rho_d$ , and  $c_1$  through  $c_5$  are constants (see Anderson (2006) for details).

## 2.2 CFGI Frozen Ground Model

The CFGI model was originally developed as a lumped model for flood forecasting in the Pacific Northwest, but it has been used in distributed models as well (De Roo et al., 2001; Van Der Knijff et al., 2010). The rationale of the CFGI method is that air temperature ultimately controls the ground temperature, but its impact is moderated by the insulating effects of any snowpack. The presence of frozen ground is determined by the frozen ground index  $F$  ( $^\circ\text{C-days}$ ), which is calculated as:

$$F_t = F_{t-1} A - T_{a,d} e^{-0.4 K_s D_s}, \quad (10)$$

where  $T_{a,d}$  is the average daily air temperature ( $^{\circ}\text{C}$ ),  $A$  is a daily decay coefficient, and  $K_s$  is the snow reduction coefficient ( $\text{cm}^{-1}$ ).  $A$  controls the persistence of the  $F$  values, and  $K_s$  controls the insulation from the snowpack. Molnau and Bissell (1983) recommended changing  $K_s$  depending on whether  $T_{a,d}$  is above or below freezing (denoted as  $K_{s,T_a>0^{\circ}\text{C}}$  and  $K_{s,T_a<0^{\circ}\text{C}}$ , respectively).

Higher values of  $F$  indicate a higher likelihood that the ground is frozen. Once  $F$  exceeds a specified threshold ( $F_{threshold}$ ), the ground is considered frozen and infiltration is restricted. Molnau and Bissell (1983) found the ground to be frozen when  $F > 83^{\circ}\text{C-days}$  and thawed when  $F < 56^{\circ}\text{C-days}$ . When  $F$  is between these values, the ground could be either frozen or thawed. It is worth noting that  $F$  does not depend on soil moisture, which is known to affect the initialization and depth of frozen ground (Kurganova et al., 2007; Willis et al., 1961).

### 2.3 RTI Snowpack Model

The RTI model makes two modifications to the TI model: (1) it ~~accounts for interception of snow by the vegetation canopy and (2) it~~ uses a radiation-derived temperature  $T_{rad}$  ( $^{\circ}\text{C}$ ) to better describe the available energy. ~~Effective precipitation  $P_{eff}$  ( $\text{m h}^{-1}$ ) is the amount of snow that reaches the ground and is calculated, and (2) it estimates spatially-varying snowpack sublimation based on solar radiation approximations.~~

$$P_{eff} = P - I + D, \quad (11)$$

where  $I$  is the snow intercepted by the canopy ( $\text{m h}^{-1}$ ), and  $D$  is the amount of previously intercepted snow that is unloaded to the ground surface ( $\text{m h}^{-1}$ ).  $I$  is calculated using a physically-based method developed and tested by Pomeroy et al. (1998) and Hedstrom and Pomeroy (1998). As implemented by Liston and Elder (2006):

$$I_t = I_{t-1} + 0.0007(I_{max} - I_{t-1})[1 - \exp(-1000 P/I_{max})], \quad (12)$$

where  $I_{max}$  is the maximum interception storage ( $\text{kg m}^{-2}$ ), which is estimated based on leaf area index ( $L_{AI}$ ) as  $I_{max} = 4.4 L_{AI}$  (Hedstrom and Pomeroy, 1998). When  $L_{AI} = 0$ ,  $P_{eff}$  is set equal to  $P$ . Unloading of intercepted snow  $D$  only occurs when  $T_a > 0^{\circ}\text{C}$  and is calculated using a simple temperature index method (Liston and Elder, 2006):

$$D = 1.61 \times 10^{-8} (T_a - 273.16) \Delta t. \quad (13)$$

The amount of snow water equivalent residing in the canopy  $S_{swec}$  (m) is then calculated as:

$$S_{swec,t} = S_{swec,t-1} + I - S_{sub} - D, \quad (14)$$

where  $S_{sub}$  (m) is the amount of snow sublimated from the canopy. Following Liston and Elder (2006),  $S_{sub}$  is calculated as:

$$S_{sub} = C_g I \phi \Delta t, \quad (15)$$

where  $C_g$  is the non dimensional canopy exposure coefficient and  $\phi$  is the sublimation loss coefficient for an ice sphere.  $C_g$  is a function of both  $I$  and  $I_{max}$  (Pomeroy and Schmidt, 1993), and  $\phi$  is calculated as a function of  $T_a$  and  $r_h$  (%) following Liston and Elder (2006).

The RTI model replaces  $T_a$  in Eq. (4) and (5) with a radiation-derived proxy temperature  $T_{rad}$  (°C). In those equations,  $T_a$  is used to conceptually represent the energy available to the snowpack.  $T_{rad}$  has a similar purpose but is intended to improve the estimation of available energy.  $T_{rad}$  is calculated by assuming that the radiation terms dominate the energy balance at the snow surface, so that outgoing longwave radiation balances the net incoming shortwave and longwave radiation (Follum et al., 2015). Thus:

$$R_{LW\uparrow} = R_{SW,net} + R_{LW\downarrow}, \quad (4611)$$

where  $R_{LW\uparrow}$  is outgoing longwave radiation,  $R_{SW,net}$  is the net incoming shortwave radiation, and  $R_{LW\downarrow}$  is the downwelling longwave radiation. The right side of Eq. (4611) represents the energy that is supplied to the snowpack via the atmosphere.  $R_{LW\uparrow}$  ( $\text{W m}^{-2}$ ) is the radiative response of the snowpack to that energy. Using the Stefan-Boltzmann Law,  $R_{LW\uparrow}$  can be written in terms of a temperature  $T_{rad}$ :

$$T_{rad} = \left( \frac{R_{SW,net} + R_{LW\downarrow}}{\varepsilon_{snow} \sigma} \right)^{1/4} - 273.15, \quad (4712)$$

where  $\varepsilon_{snow}$  is the emissivity of snow (assumed to be 0.97) and  $\sigma$  is the Stefan-Boltzmann constant.

$R_{SW,net}$  is calculated:

$$R_{SW,net} = (1 - \alpha_s)(R_{SW,0} - R_{SW\downarrow}), \quad (13)$$

where  $\varphi_r$ ,  $\varphi_{atm}$ ,  $\varphi_c$ ,  $\varphi_v$ ,  $\varphi_s$ ,  $\varphi_t$ ,  $\dots$  (18)

where  $R_{SW,0}$  is the solar constant (Liou, 2002) and  $\alpha_s$  is the albedo of the snowpack, which is calculated based on the time elapsed since the most recent snowfall and whether melt is occurring (Henneman and Stefan, 1999).  $R_{SW\downarrow}$  is the incident shortwave radiation, which is calculated:

$$R_{SW\downarrow} = R_{SW,0} \varphi_r \varphi_{atm} \varphi_c \varphi_v \varphi_s \varphi_t, \quad (14)$$

where  $R_{SW,0}$  is the solar constant (Liou, 2002).  $\varphi_r$  accounts for distance from the Earth to the sun (based on Julian day (TVA, 1972)),  $\varphi_{atm}$  accounts for atmospheric scattering (based on elevation (Allen et al., 2005)),  $\varphi_c$  accounts for absorption by clouds (based on fractional cloud cover (TVA, 1972)),  $\varphi_v$  accounts for vegetation (set equal to the vegetation transmission coefficient (Bras, 1990)),  $\varphi_s$  accounts for the slope/aspect of the terrain (based on latitude, slope, and azimuth angle (Duffie and Beckman, 1980)), and  $\varphi_t$  accounts for topographic shading (based on elevation, azimuth angle, and solar elevation angle).

$R_{LW\downarrow}$  is calculated from the contributions of the atmosphere (including clouds) and the canopy:

$$R_{LW\downarrow} = \sigma \varepsilon_a (T_a + 273.15)^4 (1.0 + 0.17 N^2) (1 - F_c) + F_c \sigma \varepsilon_c (T_{canopy} + 273.15)^4, \quad (4915)$$

where  $\varepsilon_a$  is the air emissivity (0.757 when snow is present based on Bras (1990)),  $N$  is the fractional cloud cover,  $F_c$  is the fractional canopy cover (estimated from leaf area index  $L_{AI}$  following (Liston and Elder, 2006; Pomeroy et al., 2002)),  $\varepsilon_c$  is the canopy emissivity (assumed equal to 1 following Sicart et al. (2004)), and  $T_{canopy}$  is the canopy temperature (°C) which is assumed equal to  $T_a$  following DeWalle and Rango (2008).

Formatted: Left

Because the TI model uses  $T_a$  to drive snowpack dynamics, those dynamics are only directly associated with the downwelling longwave radiation from the air, which is a component of  $R_{LW\downarrow}$ . Furthermore, the spatial variations in the available energy depend only on the variations of  $T_a$ , which are inferred from elevation.  $T_{rad}$  in the RTI model considers both  $R_{SW,net}$  and  $R_{LW\downarrow}$  and thus accounts for heterogeneity in topographic orientation and shading as well as canopy cover.

The TI model partially accounts for seasonal variation in solar radiation and snow albedo by empirically adjusting  $M_f$  as shown in Eq. (3). In the RTI model, seasonal variations in solar radiation and snow albedo are included in  $T_{rad}$ , so a constant melt factor  $M_f$  is used (Follum et al., 2015).

The TI model uses a uniform multiplication factor ( $S_{sf}$ ) that is applied to the precipitation to account for sublimation, but sublimation is known to vary spatially (Musselman, 2008; Rinehart, 2008; Veatch, 2009). Most sublimation methods depend on relative humidity and wind speed (e.g. Pomeroy, 1988; Liston and Elder, 2006), which are often unavailable in data sparse environments. However, Gustafson et al. (2010) linked differences in sublimation rates to the amount of solar radiation a location receives. In the RTI model a simple approach is used to estimate hourly sublimation rates  $S_{sub}$  (cm hr<sup>-1</sup>) as:

$$S_{sub} = S_{sub,d} \left( \frac{R_{SW\downarrow}}{R_{SW\downarrow,flat}} \right) \quad (16)$$

where  $S_{sub,d}$  (cm d<sup>-1</sup>) is the watershed-average daily maximum sublimation amount (a parameter), and  $R_{SW\downarrow,flat}$  is the daily shortwave radiation for a flat cell within the watershed on a cloud-free day. Thus, locations with higher  $R_{SW\downarrow}$  (e.g., open areas and south-facing slopes in the northern hemisphere) will have higher values of  $S_{sub}$ . The method neglects wind speed and relative humidity, but does vary sublimation rates based on spatial patterns of solar radiation.

## 2.4 modCFGI Frozen Ground Model

The CFGI model is modified in three ways to create the modCFGI model. First, the average daily proxy temperature  $\overline{T_{\alpha}} T_{rad,d}$  is used in place of  $T_{\alpha} T_{a,d}$  to represent available energy. Second, ground cover (leaf litter, woody debris, etc.) is included as an insulator in the frozen ground index, ~~and~~. And third, an option is included to estimate frost depth is calculated based on the frozen ground index. The frost depth calculation is optional because it requires soil moisture estimates and may not be needed in many hydrologic models that only require the occurrence (not depth) of frozen ground.

The CFGI uses  $T_{\alpha} T_{a,d}$  in Eq. (10) to represent the energy that is available to heat the ground surface. In the modCFGI model,  $T_{\alpha} T_{a,d}$  is replaced with  $\overline{T_{\alpha}} T_{rad,d}$ .  $\overline{T_{\alpha}} T_{rad,d}$  is calculated using  $\alpha_s$  (see Eq. (4712) and (4813)) when snow is present, and the albedo of the land cover when snow is not present. By using  $\overline{T_{\alpha}} T_{rad,d}$ , the modCFGI model is expected to better represent the spatial heterogeneity of energy supply due to variations in the topography and canopy cover within a watershed.

The insulation by the ground cover is included by modifying Eq. (10) to become:

Formatted: Condensed by 0.1 pt

$$F_t = F_{t-1}A - T_{rad} e^{-0.4(K_s D_s + K_{gc} D_{gc})}, \quad (2017)$$

where  $K_{gc}$  is the ground cover reduction coefficient ( $\text{cm}^{-1}$ ) and  $D_{gc}$  is the depth of ground cover (cm). This formulation retains the original form of the CFGI model but includes insulation from both snowpack and ground cover.  $F$  can still be used to identify the occurrence of frozen ground, which may be sufficient for many hydrologic models. However, because  $F$  is not a measurable quantity, an option to extend modCFGI to calculate frost depth is also needed.

~~The frost~~Frost depth is calculated ~~based on using  $F$  and~~ the modified Berggren Equation. As originally proposed (and described by DeWalle and Rango (2008)), ~~this~~the Berggren equation relates the number of degree days in the freezing/thawing period  $U$  ( $^{\circ}\text{C}\text{-days}$ ) to the maximum frost depth  $Z_{\max}$  (m) as follows:

$$Z_{\max} = \lambda(48 U \delta^{-1} \Omega_m)^{1/2}, \quad (2118)$$

where  $\lambda$  is a dimensionless coefficient that accounts for changes in sensible heat of the soil,  $\delta$  ( $\text{J m}^{-3}$ ) is the latent heat of fusion of the soil, and  $\Omega_m$  ( $\text{J m}^{-1} \text{h}^{-1} ^{\circ}\text{C}^{-1}$ ) is the mean thermal conductivity of the frozen and unfrozen soil layers. The derivation and corresponding assumptions (i.e. linear soil temperature gradients (Aldrich, 1956)) do not reveal any major impediments to adapting this equation for a shorter time step. In addition, Fox (1992), Woo et al. (2004), and Carey and Woo (2005) have used a layered version of the Stefan Equation, which is similar to Eq. (2118) to simulate daily frost depths with daily input data. Thus, the modified Berggren Equation is applied at a daily time scale and revised to become:

$$Z_d = \lambda[48 (F - F_{\text{threshold}}) \delta^{-1} \Omega_m]^{1/2}, \quad (2219)$$

where  $Z_d$  is the depth of frozen ground (m). By using the difference between  $F$  and  $F_{\text{threshold}}$ , the degree-days ~~from~~of the current freezing/thawing period is utilized, which is similar to the use of  $U$  in the original equation.  $Z_d$  is only calculated once the ground begins to freeze (when  $F > F_{\text{threshold}}$ ).  $Z_d$  deepens as  $F$  becomes increasingly larger than  $F_{\text{threshold}}$ . When  $F$  decreases (due to increasing  $T_{rad}$ ), so does the thickness of frost depth. No frost remains when  $F$  falls below  $F_{\text{threshold}}$ .

For the original modified Berggren Equation,  $\lambda$  can be estimated annually from Aldrich (1956) using  $U$ , the mean annual air temperature, and the soil water content  $\omega$  (% of dry weight). Here,  $\lambda$  is calculated using daily differences between  $F$  and  $F_{\text{threshold}}$ , the mean annual air temperature, and daily  $\omega$  values. Thus, soil moisture is included in the calculation of  $Z_d$  even though it is not included in the calculation of  $F$ . Furthermore,  $\delta$  is estimated daily as:

$$\delta = \delta_f \rho \omega / 100, \quad (2320)$$

where  $\delta_f$  is the latent heat of fusion of water ( $0.334 \text{ MJ kg}^{-1}$  at  $0^{\circ}\text{C}$ ) and  $\rho$  is the dry soil density.  $\Omega_m$  is estimated as (Farouki, 1981; Johansen, 1977):

$$\Omega_m = (\Omega_{\text{sat}} - \Omega_{\text{dry}})\omega + \Omega_{\text{dry}}, \quad (2421)$$

where  $\Omega_{\text{dry}}$  and  $\Omega_{\text{sat}}$  are the thermal conductivity of dry and saturated soil, respectively.  $\Omega_{\text{sat}}$  is calculated as the geometric mean of the conductivities of the materials within the soil profile (Farouki, 1981; Johansen, 1977):

$$\Omega_{\text{sat}} = \Omega_s^{(1-n_{\text{total}})} \Omega_{\text{ice}}^{(n_{\text{ice}})} \Omega_{\text{water}}^{(n_{\text{total}}-n_{\text{ice}})}, \quad (2522)$$

where  $\Omega_s$ ,  $\Omega_{ice}$ , and  $\Omega_{water}$  are the thermal conductivity of solids, ice, and water, respectively (Farouki, 1981).  $n_{total}$  is the porosity, and  $n_{ice}$  is:

$$n_{ice} = n_{total} Z_d / H, \quad (2623)$$

where  $H$  (m) is the soil thickness.

## 5 3 Model Application

### 3.1 Study Area

The TI/CFGI and RTI/modCFGI models are tested at the W-3 sub-basin (Fig. 1) of the SREW. The study period is 1 Oct 2005 through 30 Sept 2010, which is water year (WY) 2006 through 2010. The SREW was founded in 1958 primarily for studies of snow accumulation, melt, and runoff (Anderson, 1973; Anderson, 1976; Dunne and Black, 1970a; Dunne and Black, 1970b; Dunne and Black, 1971; Shanley, 2000; Shanley and Chalmers, 1999). The W-3 sub-basin is located at 44° 29' N and 72° 09' W. Elevations range between 348 m and 697 m, and the area is approximately 8.5 km<sup>2</sup> (based on the National Elevation Dataset (Gesch et al., 2002)). The basin is primarily forested with deciduous (57.7%), evergreen (7.8%), and mixed (15.3%) trees (based on the 2006 National Land Cover Database (NLCD) (Fry et al., 2011)). Approximately 14.6% of the land cover is pasture/hay and cultivated crops. These open areas are typically below an elevation of 525 m, which is the approximate limit for viable agriculture (Shanley and Chalmers, 1999). The W-3 sub-basin is extensively gaged for both hydrometeorology and hydrology by the U.S. Geological Survey (USGS) and collaborators from federal agencies and universities. Additional basin information and data are provided by Anderson et al. (1979), Shanley et al. (1995), Shanley and Chalmers (1999) and the USGS website (<https://nh.water.usgs.gov/project/sleepers/index.htm>, accessed 7 November 2016).

Two snow sites and 35 frost sites within W-3 were monitored by the Vermont Field Office of the USGS. At the snow sites, SWE and snow depth were measured approximately weekly, and both sites are used in the present study. At the frost sites, snow depth and frost depth were measured periodically (between 0 and 14 measurements in a given winter). Frost depth was measured using ~~pages described by CRREL-Gandahl frost tubes (Ricard et al., 1976)), which are filled with a methylene blue solution. The frost depth is identified by a change in colour within the tube (blue indicates thawed, clear indicates frozen).~~ Vermette and Kanack (2012) provide images and descriptions of similar frost tubes, and Shanley and Chalmers (1999) provides detailed descriptions of the frost tubes at SREW. The frost sites (labelled FS in Fig. 1) are clustered in six parts of the watershed. For this paper, one site from each cluster (FS4, FS11, FS21, FS24, FS30, and FS40) was selected for analysis. The selected sites are far enough apart to be relatively independent but still capture the variations in elevation and land cover classification within the watershed.

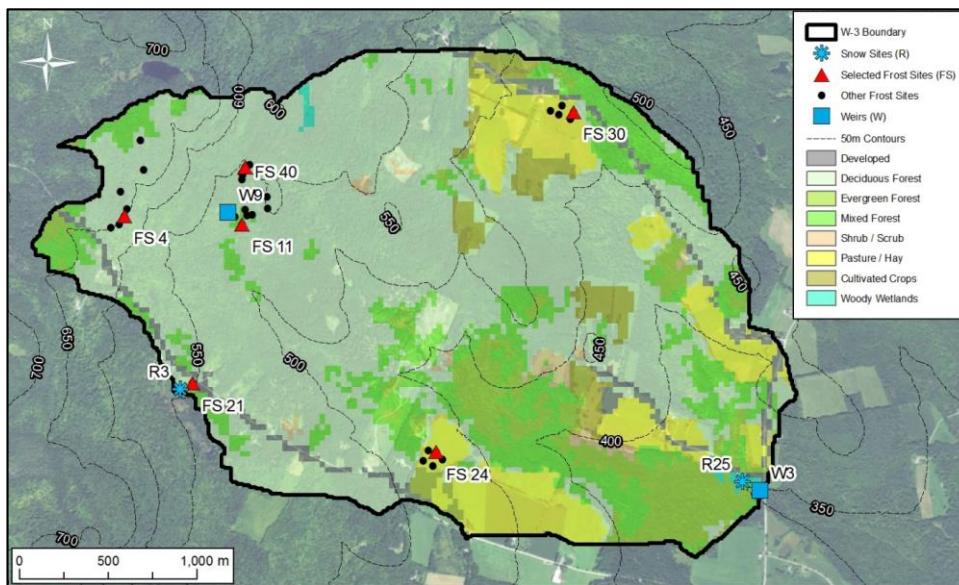


Figure 1. W-3 sub-basin in the Sleepers River Experimental Watershed. Sites used in this study are identified with red triangles and blue snowflakes. Basin delineation and elevation contours (m) are based on the 1/3-arc-second National Elevation Dataset, land cover classification based on the 2006 National Land Cover Database, and sources of the background imagery include ESRI, DigitalGlobe, Earthstar Geographics, CNES/Airbus DS, GeoEye, USDA FSA, USGS, Getmapping, Aerogrid, IGN, IGP, and the GIS User Community.

### 3.2 Model ~~Forcing Data~~Inputs

~~Hourly~~The TI and CFGI models require hourly precipitation and temperature data, which were obtained from the USGS. Precipitation was measured at the W9 weir and R3 snow site (Fig. 1). The USGS then creates a single spatially-averaged precipitation ~~timeseries~~time series by weighting the measurements using the distribution of elevation (based on personal communication with Dr. James Shanley of the Vermont Field Office of the USGS on 14 November 2016). The W9 gage receives more weight because the watershed includes elevations both above and below this site. Hourly temperature was measured at the W9 site, which has an elevation of 520 m. ~~All other hydrometeorological data~~

The RTI and modCFGI models also require cloud cover data, which were obtained from the National Centers for Environmental Information (NCEI, <https://www.ncdc.noaa.gov/>, accessed 7 November 2016). ~~Specifically, The~~ hourly ~~relative humidity, atmospheric pressure, and wind speed were obtained from the Fairbanks Museum in Saint Johnsbury, VT (11 km southeast of the basin). Hourly cloud-cover classification data were obtained from both (clear, few clouds, broken sky, etc.) were collected at~~ the Edward F. Knapp State Airport (44 km southwest of the basin) and the Morrisville-Stowe



State Airport (36 km west of the basin). The ~~cloud cover classifications (clear, few clouds, broken sky, etc.) were~~  
~~then classification data were~~ converted to cloud cover percentages using the method from Follum et al. (2015).  
~~Relative~~Cloud cover data are routinely measured at most airports in the U.S. (data archived at NCEI) as well as many  
~~meteorological stations. For simulation of frost depth (and comparison to frost depth observations), soil moisture and~~  
5 ~~evapotranspiration were also simulated. These two components additionally require hourly relative~~ humidity, ~~wind speed,~~  
~~and atmospheric pressure, and wind speed data, all of which were obtained~~ from ~~the two airports were used to replace~~  
~~missing values within a meteorological station at~~ the Fairbanks Museum dataset. ~~All of the hydrometeorological data~~  
~~described are required in long-term GSSHA simulations in Saint Johnsbury, VT (11 km southeast of the basin) with missing~~  
~~values filled-in using hourly data from the two airports.~~

10 ~~All the models require elevation data to determine the spatial patterns of snow and frozen ground.~~ W-3 was  
delineated using the 1/3-arc-second (~9 m) National Elevation Dataset (Gesch et al., 2002). ~~Land~~The RTI and CFGI models  
~~additionally require land~~ cover classifications, ~~which~~ were obtained from the 2006 National Land Cover Database (Fry et al.,  
15 ~~2011), which has) and have~~ a 30-m resolution. The classifications of some grid cells were changed to match the land covers  
observed in the field. In particular, the grid cell containing R3 was changed from deciduous forest to pasture/hay, FS11 was  
changed from mixed forest to evergreen forest, and FS21 was changed from developed to mixed forest. Both FS24 and  
FS30 are classified as pasture/hay, where FS24 is a managed pasture and FS30 is an unmanaged pasture (personal  
communication with Ann Chalmers of the Vermont Field Office of the USGS on 15 November 2016). For example, during  
field observations in November 2016, FS24 had manure spread throughout the field, while FS30 was not fertilized. ~~Soil~~  
~~classifications~~

20 ~~Soil classification data are also required if calculating frost depth, which~~ were obtained from the Digital General  
Soil Map of the United States (Soil Survey Staff, Natural Resources Conservation Service, United States Department of  
Agriculture, Web Soil Survey, available online at <http://websoilsurvey.nrcs.usda.gov/>. Accessed 10 August 2016). Almost  
the entire W-3 basin is classified as fine sandy loam. The Watershed Modeling System (Aquaveo, 2013) was used to  
develop the GSSHA model with a 30-m structured grid. This resolution is adequate to capture the spatial heterogeneity of  
25 the basin while remaining computationally efficient.

### 3.3 Parameter Estimation and Calibration

The Model-Independent Parameter Estimation and Uncertainty Analysis (PEST) method (Doherty et al., 1994) was  
used to calibrate ~~the models, 7 parameters in the TI model and 8 parameters in the RTI model.~~ PEST is a nonlinear local  
search parameter estimator that calibrates numerous parameters simultaneously to produce the best fit between simulated  
30 results and observations. WY 2006 and 2007 were used as the calibration period. The TI and RTI snow models were  
calibrated first to minimize the sum of the squared residuals between simulated and observed snow depths at the 8 sites (6  
frost sites and 2 snow sites).

Table 1 displays the allowable range, calibrated value, and sensitivity ranking for the calibrated snow parameters. Goodness of fit statistics as well as description of affects each parameter has on the snow simulations are described in the Results and Discussion section. The allowable ranges for  $A_{TIPM}$ ,  $f_u$ ,  $L_{hc}$ ,  $N_{mf,max}$ ,  $M_f$ ,  $M_{f,max}$ , and  $M_{f,min}$  are based on physical limitations and typical ranges in the literature (Follum et al., 2014,2015).  $L_{AI}$  can be estimated from seasonal and annual relationships to remotely-sensed normalized difference vegetation index (NDVI) values (Wang et al., 2005). However, snowpack affects the measurement of greenness in high latitude regions (Beck et al., 2006). Thus,  $L_{AI}$  was calibrated for each land cover classification using feasible ranges based on Liston and Elder (2006). Because the seasonal snowpack typically occurs after leaves have fallen, the minimum values of  $L_{AI}$  for each land cover type from Liston and Elder (2006) are considered. Separate  $L_{AI}$  and  $K_v$  values were calibrated for based on land cover classifications with forested land covers being categorized as deciduous forest (including deciduous forest, woody wetlands, and mixed forest), or evergreen forest, and pasture (including pasture/hay, cultivated crops, and shrub/scrub).  $L_{AI}$  and  $K_v$  values for non-forested land cover classifications were set to 0.0 and 1.0, respectively.  $T_{px}$  and  $T_{mbase}$  were not calibrated (both are 0°C) because the temperature data were post-processed by the Vermont USGS and are expected to be accurate. By comparing the temperature measurements at W9 and the Fairbanks Museum (elevation of ~212.4 m),  $\phi$  was estimated at 6.6 °C km<sup>-1</sup>. All snow density parameters are set constant based on Anderson (1973) and Anderson (2006).

The PEST results indicate that the TI model's snow depths are most sensitive to the melt factors ( $M_{f,min}$  and  $S_{cf}$ ,  $M_{f,max}$ ,  $A_{TIPM}$ , and  $M_{f,min}$ ). For the RTI model, snow depths are most sensitive to vegetation related parameters including  $K_v$  for the open pasture sites and (deciduous),  $A_{TIPM}$ ,  $L_{AI}$  for the deciduous forest sites (evergreen), and  $M_f$  (Table 1). The calibrated pasture  $L_{AI}$  deciduous  $K_v$  is at near the top of the allowable range (1.0,250). Higher  $L_{AI}$  values produce decreased snowpack due to greater interception) and  $R_{eq}$  values. Thus, the calibration is clearly attempting to match low snowpack levels at the pasture site. One potential cause for the low snowpack at this site is  $L_{AI}$  is near the bottom (0.103), indicating that the snow transport by wind in open the deciduous forest behaves similarly to the open pasture areas, which is not included in either of the snow models considered here where  $K_v=1$  and  $L_{AI}=0$ .

Table 1. Allowable ranges and calibrated values for the TI and RTI model parameters using PEST. Dashes indicate parameters that are not required in the associated model. The sensitivity ranking for each parameter is shown in parentheses.

Parameter	Units	Allowable Range	Calibrated Values	
			TI	RTI
$M_{f,max}$	mm °C <sup>-1</sup> (6 h) <sup>-1</sup>	0.001-2.400	1.940017 (2)	--
$M_{f,min}$	mm °C <sup>-1</sup> (6 h) <sup>-1</sup>	0.001-1.600	1.600 (+0.001 (4))	--
$M_f$	mm °C <sup>-1</sup> (6 h) <sup>-1</sup>	0.001-2.400	--	1.080 (30.391 (4))
$S_{cf}$	fraction mm °C <sup>-1</sup> (6 h) <sup>-1</sup>	0.001-2.400	0.001 (4869 (1))	--
$N_{mf,max}$	mm °C <sup>-1</sup> (6 h) <sup>-1</sup>	1.000	--	0.130 (8)

Formatted: Comment Reference

<del><math>f_{sub,d}</math></del>	<del><math>\text{mm-mb cm d}^{-1} (6 \text{ h})^{-1}</math></del>	0.001- <del>1.000</del> 0.100	<del>0.500 (6)</del>	<del>0.500 (11068)</del> (6)
<del><math>N_{inf}</math></del>	<del><math>\text{mm } ^\circ\text{C}^{-1} (6 \text{ h})^{-1}</math></del>	0.001- <del>1.000</del> 2.400	<del>1.000</del> (30.002 (6)	<del>0.985 (7256)</del> (8)
<del><math>\max_{t_{decid}}</math></del>	<del><math>\text{mm mb}^{-1} (6 \text{ h})^{-1}</math></del>	0.001- <del>0.100</del> 1.000	<del>0.001</del> (5500 (7)	<del>0.001500</del> (10)
<del><math>L_{decid}</math></del>	<del><math>\text{fraction}</math></del>	0.200001- <del>1.000</del>	<del>0.545 (4992)</del> -1.000 (3)	<del>0.545 (4992)</del> (2)
<del><math>K_{v,pasture}</math></del>	<del><math>\text{fraction}</math></del>	<del>0.800</del> <del>1.000</del> 0.001	<del>0.800 (4001)</del> 0.100	<del>0.800 (4001)</del> (9)
<del><math>K_{v,evergreen}</math></del>	<del><math>\text{fraction}</math></del>	0.200- <del>0.800</del> 1.000	<del>0.305 (9969)</del> --	<del>0.305 (9969)</del> (1)
<del><math>L_{decid}</math></del>	<del><math>\text{fraction}</math></del>	0.400- <del>1.000</del> 2.00	<del>1.000</del> 0.800	<del>1.000</del> (20.308 (7)
<del><math>K_{v,evergreen}</math></del>	<del><math>\text{fraction m}^2 \text{ m}^{-2}</math></del>	0.001- <del>0.250</del> 1.00	<del>0.250 (103)</del> 1.000	<del>0.250 (103)</del> (5)
<del><math>L_{AI}</math></del>	<del><math>\text{m}^2 \text{ m}^{-2}</math></del>	1.000-4.000	--	1.000 (63)

Formatted Table

Formatted Table

The CFGI and modCFGI frozen ground models were calibrated to minimize the sum of squared residuals between the simulated and observed frost depths at the 6 frost sites. For purposes of comparison the modified Berggren equation was also added to the CFGI model to calculate frost depth. Table 2 displays the allowable range, calibrated value, and sensitivity ranking of each calibrated frozen ground parameter. Goodness of fit statistics as well as description of affects each parameter has on the frost depth simulations are described in the Results and Discussion section.  $F_{threshold}$  was calibrated for both the CFGI and modCFGI models with the upper range based on Molnau and Bissell (1983). Three  $K_{gc}$  values were calibrated for the modCFGI frozen ground model: one for the managed pasture site FS24 ( $K_{gc,FS24}$ ), one for the unmanaged pasture site FS30 ( $K_{gc,FS30}$ ), and one for ~~the forested~~all other frozen ground sites ( ~~$K_{gc,forest}$~~  $K_{gc}$ ).

Following Molnau and Bissell (1983), multiple combinations of  $A$  (0.8 and 0.97), and  $K_{s,T_a < 0^\circ\text{C}}$  and  $K_{s,T_a > 0^\circ\text{C}}$  (0.08, 0.2, and 0.5) values were tested with  $A = 0.97$ ,  $K_{s,T_a < 0^\circ\text{C}} = 0.08$ , and  $K_{s,T_a > 0^\circ\text{C}} = 0.5$  producing frost indices that best replicate the rise and fall of the frost depth as well as the timing of the peak frost depth. Depth of ground cover for each land cover type was obtained from field observations in November 2016. Specifically,  $D_{gc} = 6$  cm for deciduous forest (fallen leaves),  $D_{gc} = 2$  cm for evergreen forest (fallen leaves),  $D_{gc} = 4$  cm for pasture (grass), and  $D_{gc} = 0$  cm for all other land cover types.

The modified Berggren Equation requires soil moisture, which can be simulated using several methods in GSSHA (Downer and Ogden, 2006). To facilitate extension of these results to other hydrologic models, the commonly-used single-layer Green and Ampt infiltration model (Green and Ampt, 1911) with soil moisture redistribution between rainfall events

(Ogden and Saghafian, 1997) is utilized to calculate infiltration. Soil moisture is tracked using a simple bucket approach, accounting for infiltration, evapotranspiration, and groundwater recharge as described in Downer (2007). The soil layer thickness ( $H$ ) is set to 0.5 m for both the soil moisture calculations and frost depth equations. Soil infiltration parameters are set based on published values for the W-3 soil type (Downer and Ogden, 2006; Rawls et al., 1982; Rawls and Brakensiek, 1985; Rawls et al., 1983) and are shown in Table 3. Evapotranspiration, which can reduce the soil moisture, is simulated using a Penman Monteith approach (Monteith, 1965; Monteith, 1981) with parameters estimated based on land cover (Downer and Ogden, 2006). The dry soil density ( $\rho = 1137 \text{ kg m}^{-3}$ ) and dry soil thermal conductivity ( $\Omega_{dry} = 792 \text{ J m}^{-1} \text{ h}^{-1} \text{ }^{\circ}\text{C}^{-1}$ ) are set based on measurements of fine sandy loam by Nikolaev et al. (2013).

For the CFGI model, the calibrated  $F_{threshold}$  value (Table 2) is relatively close to the lower bound value of 56°C-days found in Molnau and Bissell (1983). For the modCFGI model, the calibrated  $F_{threshold}$  value is at the lower bound. The  $F_{threshold}$  value is expected to be lower for the modCFGI model than the CFGI model. The modCFGI model incorporates the insulation by ground cover directly using  $K_{gc}$  and  $D_{gc}$ , whereas the CFGI model can only account for those effects by adjusting the  $F_{threshold}$  value. It is also worth noting that  $K_{gc,FS30}$  has a very low value (minimum of allowable range), which suggests that insulation from grass in an unmanaged pasture is very small. This could be the result of snow falling within the grass of the unmanaged pasture, thus making any insulating contribution from the grass very small.

20

**Table 2. Allowable ranges and calibrated values for the CFGI and modCFGI model parameters using PEST. Dashes indicate parameters that are not required in the associated model. The sensitivity ranking for the modCFGI parameters are shown in parentheses.**

Parameter	Units	Allowable Range	Calibrated Values	
			CFGI	modCFGI
$F_{threshold}$	$^{\circ}\text{C} - \text{days}$	<del>40</del> 5.00-83.00	<del>40</del> 52.55	<del>40</del> 5.00 (23)
$K_{gc}$	cm	0.001-1.000	--	<del>0.719</del> 1.033 (1)
$K_{gc,FS24}$	cm	0.001-1.000	--	<del>1.000</del> (3887 (2)
$K_{gc,FS30}$	cm	0.001-1.000	--	0.001 (4)

25 **Table 3. Values of soil parameters used to calculate soil moisture in the single-layer Green and Ampt infiltration model.**

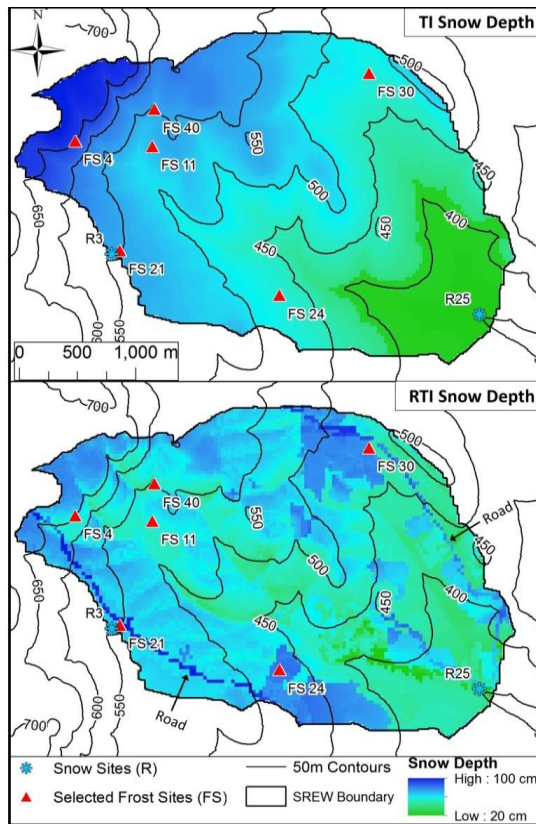
Parameter	Units	Value
<i>saturated hydraulic conductivity</i>	$\text{cm h}^{-1}$	2.040
<i>effective porosity</i>	$\text{cm}^3 \text{ cm}^{-3}$	0.407

<i>residual <del>saturation</del>water content</i>	$\text{cm}^3 \text{ cm}^{-3}$	0.038
<i>field capacity</i>	$\text{cm}^3 \text{ cm}^{-3}$	0.166
<i>wilting point</i>	$\text{cm}^3 \text{ cm}^{-3}$	0.075
<i>capillary head</i>	cm	8.570
<i>pore distribution arithmetic mean</i>	$\text{cm cm}^{-1}$	0.466

#### 4 Results and Discussion

##### 4.1 Snow Depth and SWE (TI vs RTI)

Figure 2 shows maps of simulated snow depth on 23 February 2007 from the TI and RTI snow models. The spatial variability in the TI snowpack is entirely based on elevation (due to the inference of local air temperature from elevation). Higher elevations have deeper snowpack due to lower air temperatures. The RTI snowpack also varies with elevation but ~~also includes~~shows variation due to land cover as well. In particular, pasture areas have ~~deeper~~slightly shallower snowpack than surrounding areas due to ~~lower interception/higher~~ sublimation rates and ~~lower  $R_{diff}$~~ higher absorbed shortwave radiation. North-facing slopes also have more snow than south-facing slopes due to lower  ~~$R_{sw,net}$~~ absorbed shortwave radiation. Although no maps of observed snow depth are available for comparison, large-scale distributions of snowpack are known to be controlled by elevation, land cover, and slope/aspect (Fassnacht et al., 2017; Jost et al., 2007), which is more consistent with the RTI model.



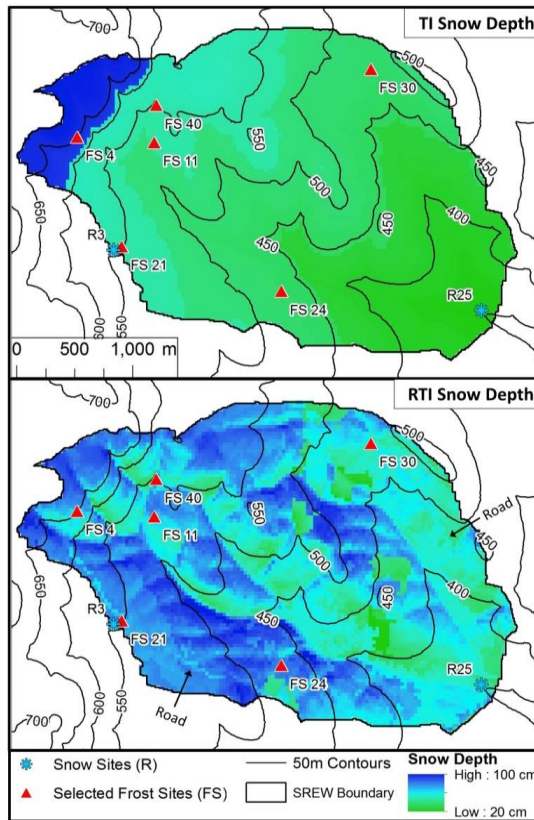
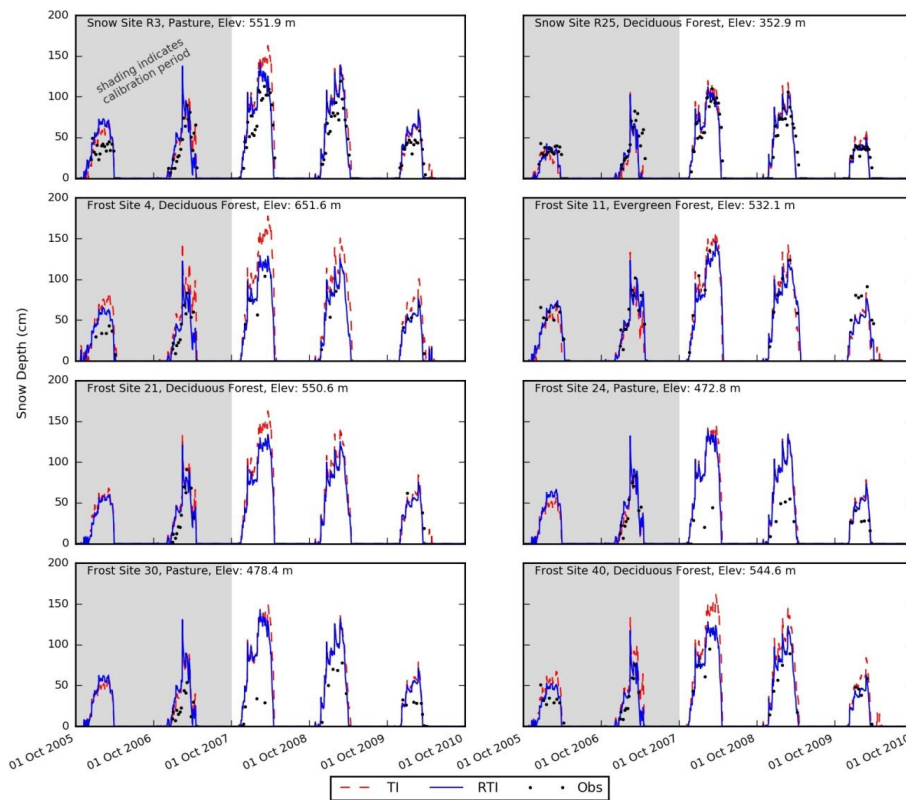


Figure 2. Simulated maps of snow depth (TI and RTI models) within the W-3 watershed for 23 February 2007. No observed maps of snow depth are available, but the map shows the differences between the temperature-based (TI) model and the modified (RTI) model.

Figure 3 shows the snow depths from the TI and RTI models at all 8 test locations and compares them to the observations. Root mean squared error (RMSE) and Nash-Sutcliffe Efficiency (NSE) are shown in Table 4 for the calibration period (WY 2006-2007), validation period (WY 2008-2010), and complete period (WY 2006-2010). The TI and RTI models track closely together at the 8 test locations despite differences in the snow depth shown in Fig. 2. The test sites are typically located on shallow slopes where terrain has limited influence on the energy available to melt the snowpack. Therefore, differences between the TI and RTI snowpack at the test sites are more related to the effects of vegetation. In Fig. 3, the two models tend to produce similar results at the pasture sites (see FS24, FS30, and R3), but they tend to differ at the deciduous forest sites (see FS4, FS21, and FS40). At the deciduous sites the RTI model often produces lower peak

Formatted: Indent: First line: 0.5"

snowpack due to the interception and sublimation of snowpack by the canopy (which are not included in the TI model). Overall, the RTI model performs better than the TI model (lower RMSE values and higher NSE values in Table 4), suggesting that inclusion of sublimation/interception and use of  $T_{\text{air}}$  improve the spatial representation of the snowpack. Differences between the TI and RTI snowpack at the test sites are small (Fig. 3 and Table 4). The RTI model performs slightly better than the TI model in overall average RMSE (15.69 vs. 15.71 cm), while the TI model performs slightly better in overall average NSE (0.58 vs. 0.53). The observed snow depth is relatively low in WY2008 and 2009 at two of the pasture sites (FS24 and FS30) compared to the other sites. ~~These two years of~~ Specifically in WY2008 the small snow depth observations are not captured within either model. The R3 site is also classified as pasture yet has a higher snowpack in WY2008 and 2009. The higher snowpack at this pasture site may be explained by the proximity of R3 to forested areas, which may reduce the wind and help preserve the snowpack. Neither model considers wind effects.





The snow depths from the two models are similar at each location (Fig. 3) because on average the available energy to melt snow ( $T_a$  in the TI model and  $T_{rad}$  in the RTI model) is similar (Fig. 4). However, the diurnal variation of  $T_{rad}$  is typically greater than that of  $T_a$ .  $T_{rad}$  is derived from a simple radiation balance (i.e. neglecting other terms in the thermal energy balance). Thus,  $T_{rad}$  is higher than  $T_a$  during the day due to high  $R_{SWI}$  values, and it is typically lower than  $T_a$  at night because  $R_{SWI}$  reduces to 0 and  $\varepsilon_a$  (set to 0.757) in Eq. (15) limits the affect  $T_a$  has on  $R_{LWI}$  and therefore  $T_{rad}$ . As shown in Fig. 4, the available energy is also similar between these locations. The elevation difference between the highest and lowest elevation site is approximately 300 m, corresponding to a maximum temperature difference of approximately 2°C between the sites. Also, the test sites are typically located on shallow slopes so topographic aspect has little influence on the energy available to melt the snowpack (i.e.  $T_{rad}$ ). All land cover classifications except evergreen forest (FS11) have  $K_v$  values at or near 1 and  $L_{AI}$  values at or near 0, which reduces any variations due to land cover.  $T_{rad}$  at FS11 (evergreen forest) is different from the other 7 sites because its low  $K_v$  value (0.308) reduces  $R_{SW,net}$  during the day, and a high  $L_{AI}$  value (1.0) increases  $R_{LWI}$  during day and night.

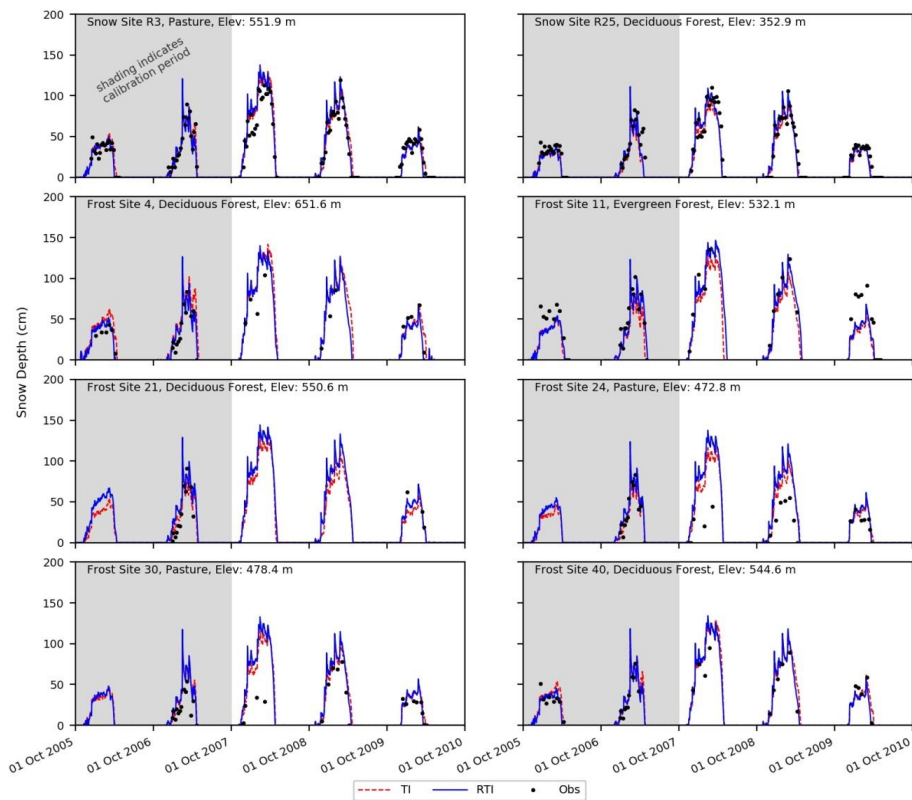


Figure 3. TI and RTI simulated snow depth at all eight test sites within the W-3 watershed.

[illegible]Snow Depth

R25	Deciduous Forest	TI	7.5.2	-	42.7	0.779	5.83.7	0.588
			0.472	2		2	3	
	RTI		7.1.5	-	4.63.1	0.799	5.53.8	0.628
			0.323	5		1	2	

- Formatted: English (U.K.)
- Formatted: English (U.K.)
- Formatted: English (U.K.)
- Formatted: English (U.K.)
- Formatted: English (U.K.)
- Formatted: English (U.K.)
- Formatted: English (U.K.)
- Formatted: English (U.K.)
- Formatted: English (U.K.)
- Formatted: English (U.K.)

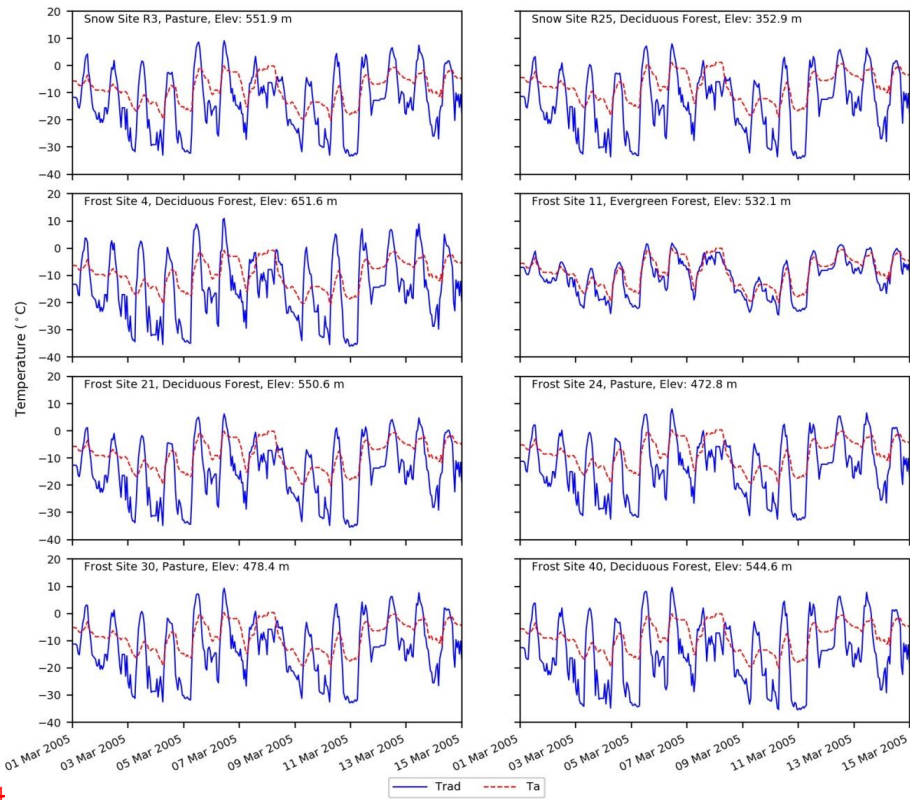


Figure 4

Figure 4.  $T_a$  and  $T_{rad}$  values at all eight test sites within the W-3 watershed between 01 March 2005 and 15 March 2005.

Figure 5 shows the simulated (both TI and RTI models) and observed SWE values, and Table 4 shows the associated performance metrics at the R3 and R25 snow sites. The TI and RTI models are only calibrated to snow depth, but SWE is calculated first and then combined with snow density to determine snow depth. Both models use the same method to

calculate snow density. Both models exhibit similar behaviour and performance at the two sites, which is consistent with their similar snow depths discussed earlier (Fig. 3 and Table 4). ~~The TI model's overestimation of SWE at R3 during WY 2008 is associated with a similar overestimation of snow depth.~~ Overall, these suggest that the snow density equations used within GSSHA are relatively accurate at the W-3 watershed. Thus, accurate estimates of snow depth typically correspond to accurate estimates of SWE as well.

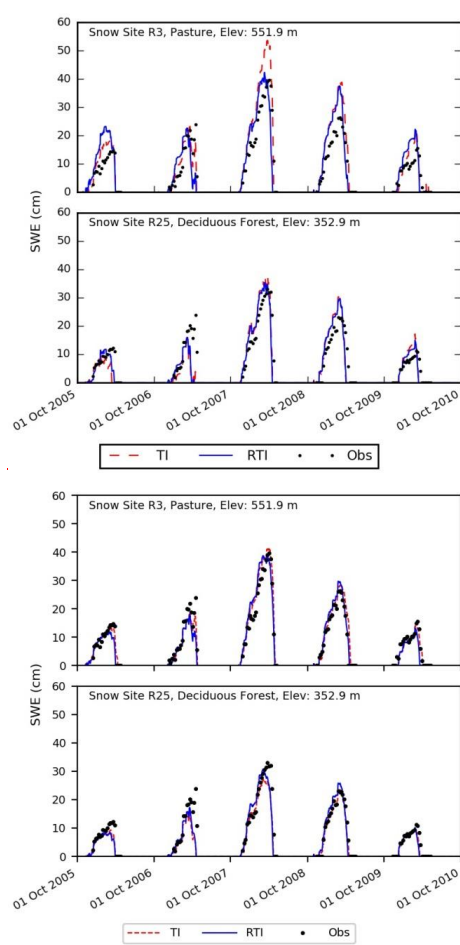
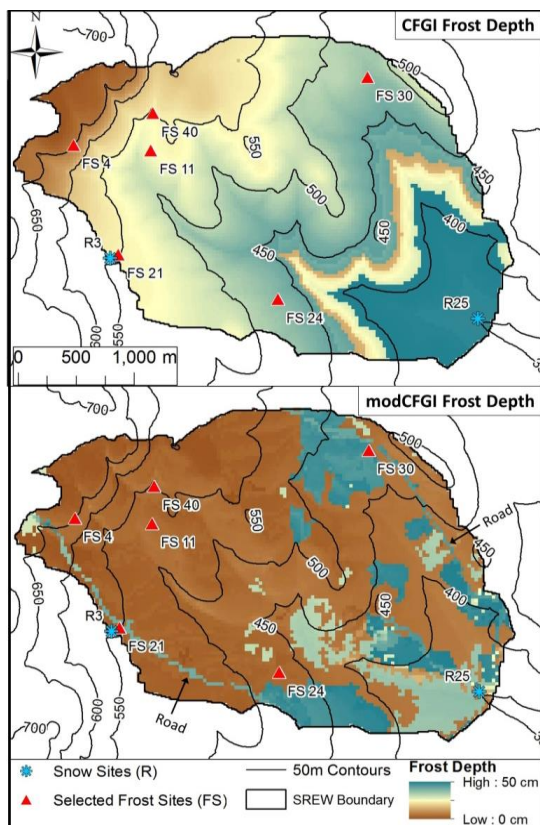


Figure 45. TI and RTI simulated SWE at R3 and R25 snow sites within the W-3 watershed.

## 4.2 Frost Depth (CFGF vs modCFGF)

Figure 56 shows simulated frost depth maps for 23 February 2007 using the CFGF and modCFGF models (no maps of observed frost depths are available for comparison). In the CFGF model, the frost depths mainly depend on elevation. Colder temperatures at higher elevations generally result in greater snowpack, which insulates the ground and produces smaller frost depths. However, at the beginning of the snow season when the snowpack is shallow, low temperatures at high elevations create deep frost in the higher elevations of the watershed. Later, deeper snowpack at high elevations insulate the ground, while the frost depth increases at lower elevations. This reversal in the elevation dependence can produce an inversion (localized minima in frost depth), as seen between the 400500 and 450650 m contour lines in Fig. 56. The modCFGF frost depth also has some elevation dependence, but ~~it shows much more the~~ spatial variation ~~mainly follows land cover classification, which is similar to observations of frozen ground in the Swiss pre-alpine zone (Stähli, 2017).~~ This variation is partly due to the use of  $T_{rad}$  and the increased heterogeneity in the snow depth. The effect of snowpack can be seen by comparing hillslopes with the same land cover but different orientations, such as along the 500 m contour south of FS11. Lower  $T_{rad}$  values on northeast-facing slopes result in deeper snowpack than the southwest-facing slopes (Fig. 2). This deeper snowpack produces shallower frost depths on the northeast-facing slopes due to insulation by the snow. However, the spatial pattern of frost depth is more heavily affected by the land cover. Land cover's impact largely occurs through the associated ground cover. This effect can be seen by comparing the deep frost at the unmanaged pasture (near FS30) with the shallower frost depth at the deciduous forest areas near FS4, FS21, and FS40. The low ground cover reduction coefficient at the unmanaged pasture ( $K_{gc,FS30}$ ) reduces the insulation from the ground cover, creating deeper frost compared to the deciduous forest areas. The larger than expected role of ground cover in the modCFGF model may occur because ground cover is present during the initiation, deepening, and decrease of frost depth, while the snowpack is much more variable throughout the season.



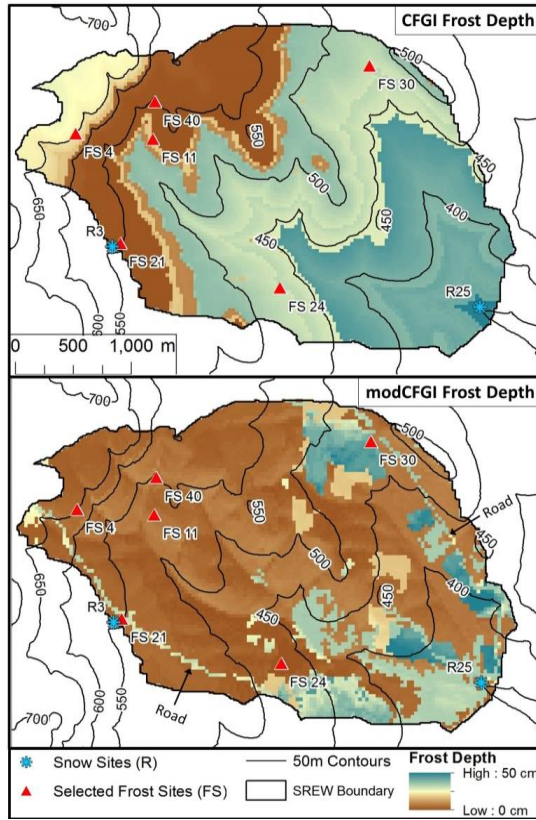


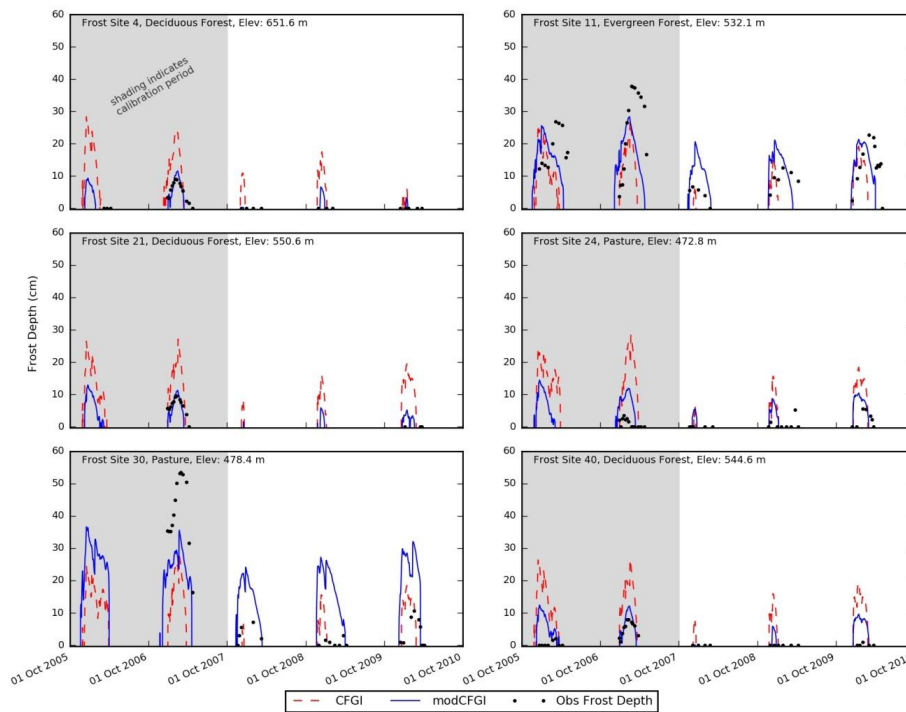
Figure 56. Simulated maps of frost depth (CFGF and modCFGF models) within the W-3 watershed for 23 February 2007. No observed maps of frost depth are available, but the map shows the differences between the temperature-based (CFGF) model and the modified (modCFGF) model.

5

Figure 67 shows the frost depths from the CFGF and modCFGF models along with the frost depth observations. The RMSE and NSE values during the calibration, validation, and overall periods are shown in Table 5. The simulated frost depth remains more constant amongst the sites when using the CFGF model, which produces similar maximum frost depths for a given year independent of the land cover. The modCFGF results deviate considerably from the CFGF results, producing greater frost depths at the unmanaged pasture (FS30) and evergreen (FS11) sites and smaller frost depths at the deciduous (FS4, FS21, and FS40) and managed pasture (FS24) sites. These simulated differences between the sites are consistent with the observations. The decreased frost depth in the deciduous forest and managed pasture result from their high measured litter depth ( $D_{gc} = 6$  cm) and high reduction coefficient ( $K_{gc,FS24} = 1.9887 \text{ cm}^{-1}$ ), respectively. The two pasture sites (FS24



and FS30) differ considerably in the observed frost depth with FS30 consistently having deeper frost. This difference likely occurs because FS24 is managed and FS30 is not. With the exception of the validation period at FS30, the modCFG model performs better (lower RMSE and higher NSE values) than the CFGI model. The difference in performance is most pronounced at the deciduous sites (FS4, FS21, and FS40) where the average overall NSE value is  $-7.26$  for the CFGI model and  $-0.49$  for the modCFG model.



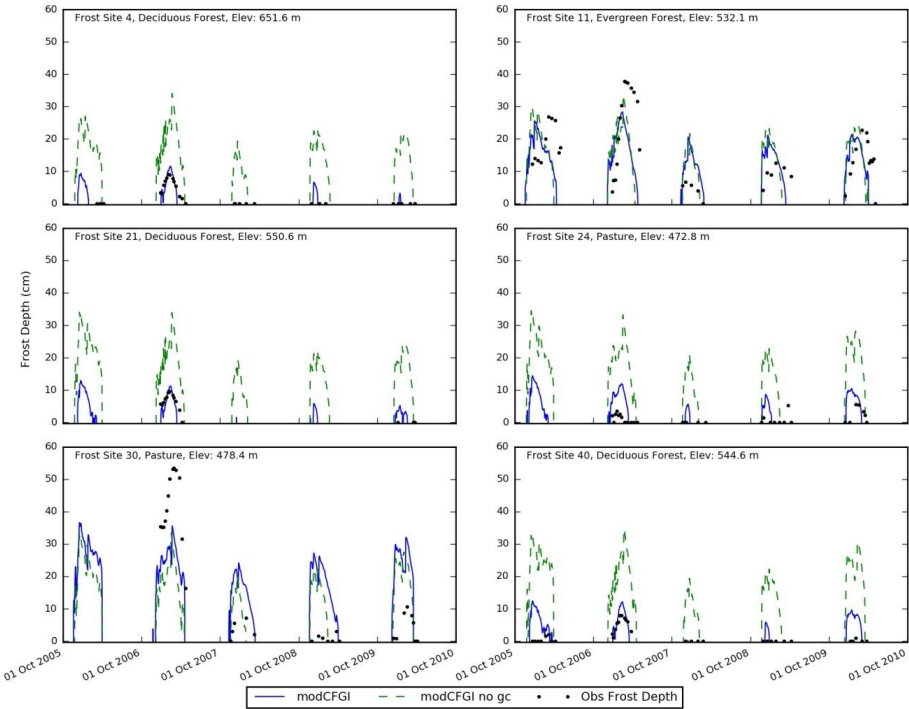


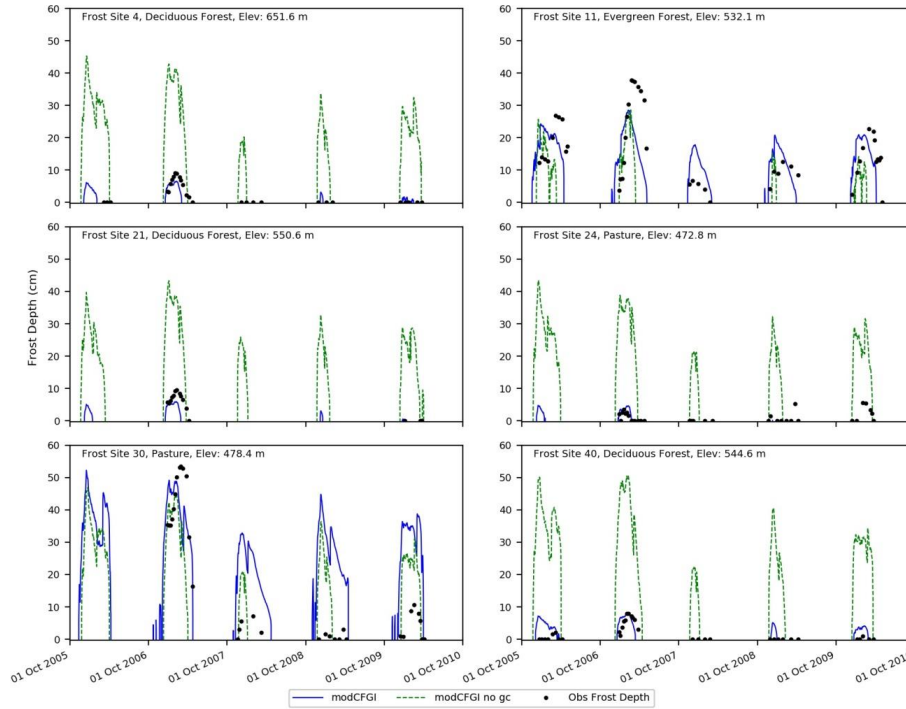




change indicates that ground cover has a large impact on the appropriate value of this threshold. Figure 78 shows the simulated frost depths using the modCFGI model with and without ground cover for each test site. Performance metrics for the modCFGI model with and without ground cover are shown in Table 5. Variability in frost depth between the sites is diminished when ground cover is removed, leading to large errors between simulated and observed frost depth. When ground cover is removed, the frost depth results decrease in accuracy (higher RMSE values and lower NSE values) compared to the complete modCFGI model. The only exception is the validation period at FS30, which is also the only site and time period when where the CFGI model outperforms the full modCFGI model. This result suggests These results suggest that the inclusion of ground cover is an important reason why the modCFGI model outperforms the CFGI model.

10

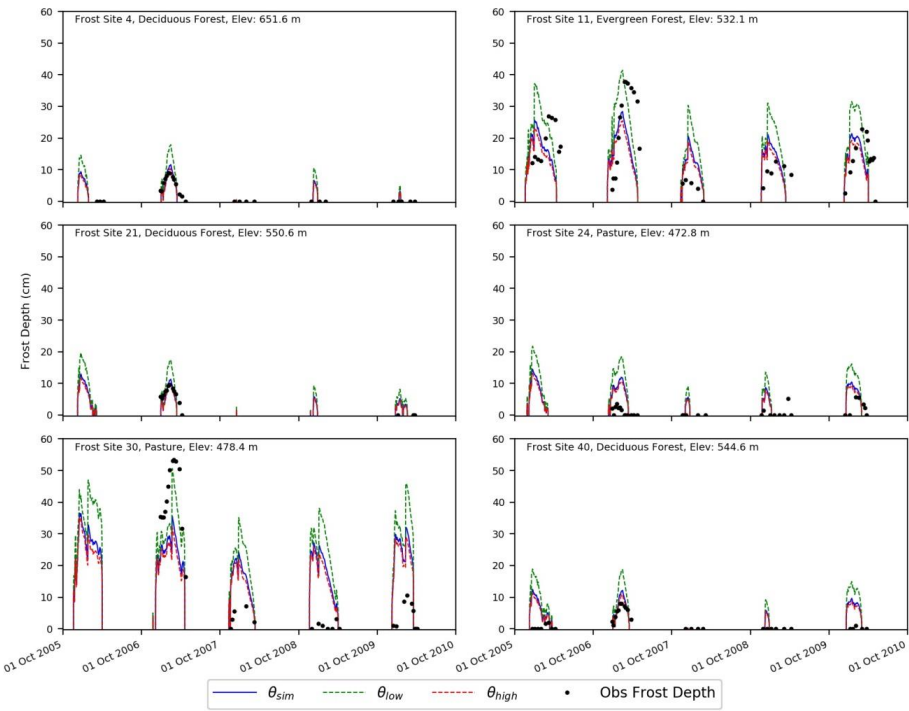




**Figure 78.** Observed frost depth compared against simulated (modCFGl with and without ground cover included) frost depth at all 6 selected frozen ground test sites within the W-3 watershed. The modCFGl model without ground cover is labelled as “modCFGl no gc”.

The sensitivity of the modCFGl results to soil moisture is also examined. Soil moisture does not affect the calculation of  $F$ , but it is included within the modified Berggren Equation (Eq. (2418) and (2219)) in the calculation of  $\delta$  (Eq. 2320) and  $\Omega_m$  (Eq. 2421). Soil moisture was simulated using a single layer Green and Ampt approach. However, no soil moisture measurements are available at any of the test sites to evaluate the accuracy of the simulated values. Sensitivity of the modCFGl model to volumetric soil moisture is tested by artificially setting the soil moisture to either the residual ~~soil~~ moisture water content ( $\theta_{low}$ ) or the effective porosity ( $\theta_{high}$ ), which are the lower and upper bounds for soil moisture values within the model. Figure 89 shows the modelled frost depths from the modCFGl model using  $\theta_{low}$ ,  $\theta_{high}$ , and the soil moisture from the Green and Ampt approach ( $\theta_{sim}$ , which is identical to modCFGl in Fig. 67 and Fig. 78). Also shown are the observed frost depths for reference only. The frost depth from the  $\theta_{sim}$  case is similar to the frost depth from the  $\theta_{high}$  because the simulated soil moisture is usually close to the effective porosity. Frost depth increases when  $\theta_{low}$  is used, which coincides with other studies (Fox, 1992; Willis et al., 1961). The timing of the frozen ground (when it begins and ends) is

identical in all three of the simulations. The consistent timing occurs because soil moisture is not used to calculate  $F$  and the same  $F_{threshold}$  (which controls when frozen ground begins) was used for all three simulations. This result highlights a deficiency in the modelling framework. Specifically, soil moisture should be considered for determining the initiation of frozen ground because wet soils have a higher specific heat capacity and require more energy loss to cool and freeze the soil (Kurganova et al., 2007).



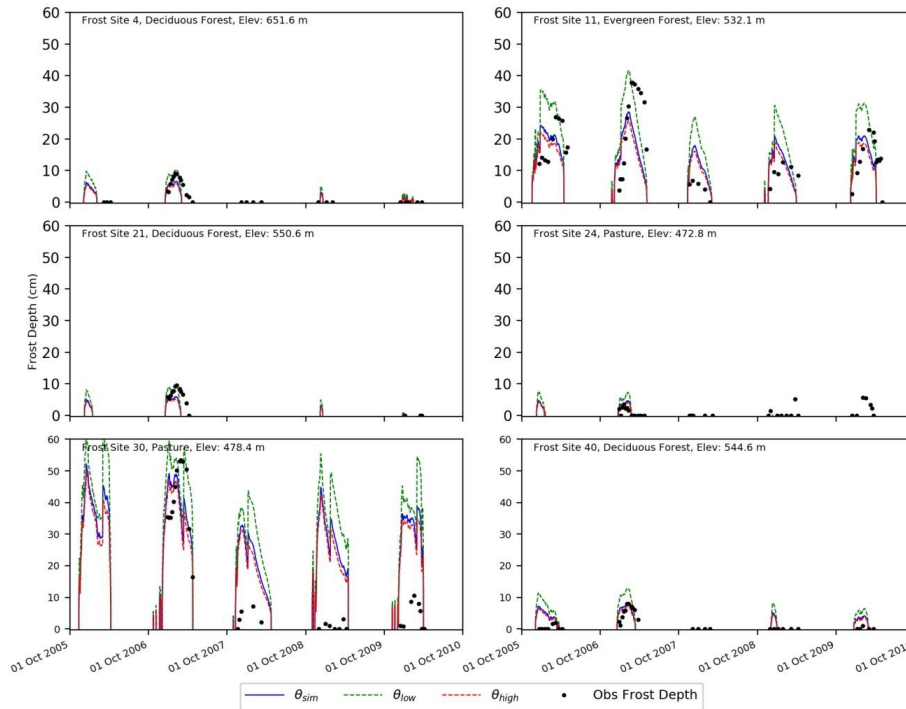


**Figure 89.** Simulated frost depths from the modCFG model using simulated soil moisture ( $\theta_{sim}$ ), a constant high soil moisture ( $\theta_{high}$ ), and a constant low soil moisture ( $\theta_{low}$ ) at all 6 selected frozen ground test sites within the W-3 watershed.

## 5 Conclusions

5 The main purpose of this paper was to better estimate the spatial pattern of frozen ground for distributed watershed modelling by modifying an existing degree-day frozen ground model (CFG), which uses a frost index value to determine whether the ground is frozen or not. The modifications to the CFG model include: 1) use of a radiation-derived temperature index (RTI) snow model instead of a standard temperature-index (TI) snow model, 2) use of a radiation-derived proxy temperature ( $T_{rad}$ ) instead of air temperature ( $T_a$ ) in the calculation of the frost index, 3) inclusion of ground cover (litter, debris, grass, etc.) as an insulator of the ground from air temperatures, and 4) implementation of an option to use a version of the modified Berggren Equation to calculate frost depths based on the frost index values. The CFG and modCFG models were tested using the GSSHA hydrologic model over a five-year period within the W-3 watershed, which is part of Sleepers River Experimental Watershed in Vermont. The model results were compared against snow depth at eight sites, snow water equivalent at two sites, and frost depth at six sites. The primary conclusions of the paper are as follows:

10



- 1.) The RTI snow model produces much more complex spatial patterns of snow depth than the TI snow model for the W-3 watershed. The TI model, which is based on SNOW-17 (Anderson, 2006), only produces spatial variation using elevation. The RTI model accounts for elevation, hillslope orientation, canopy shading, and longwave radiation from the canopy through the use of the radiation-derived proxy temperature. It also includes ~~snow interception/a simple~~ sublimation by the canopy method based on solar radiation. Thus, its snow depths exhibit spatial heterogeneity based on elevation, slope/aspect, and land cover, all of which are known to affect the largescale distribution of observed snow depths (Fassnacht et al., 2017; Jost et al., 2007).
- 2.) ~~The Both the~~ RTI model ~~produces more and TI model produce~~ accurate ~~estimates of snow depth than the TI model results~~ for the eight snow depth sites at W-3. ~~Follum et al. (2015) previously compared Two of the TI and RTI models for sites in Colorado that had the same land cover but diverse eight sites also measure snow water equivalent, where the RTI and TI model also show similarly accurate results. The eight test sites have similar topographic attributes (e.g., aspect, slope, and topographic shading). Here, the test sites and primarily differ in their land cover covers, which include pasture, deciduous forest, and evergreen forest. The RTI model more accurately simulates the Because the leaves have typically fallen prior to snow depth accumulation, all eight sites, but both models perform poorly at two of the three pasture sites. This poor performance may occur because neither model accounts for wind effects but the evergreen site behave similarly in snow accumulation and ablation.~~
- 3.) The modCFGF frost model produces more complex spatial patterns of frost depth than the CFGF frost model for the W-3 watershed. The CFGF model uses elevation to infer the spatial variation of air temperature. It also uses the TI model for snow depth, which also depends on elevation. Thus, the simulated frost depths at W-3 primarily reflect the watershed elevations. In contrast, the modCFGF model uses the radiation-derived proxy temperature to infer the energy available to heat the ground and the RTI model to simulate snow depth. Furthermore, it accounts for the insulating effects of ground cover (in addition to snowpack), which also depends on the land cover. Thus, the frost depths simulated by the modCFGF model at W-3 depend on the local elevation, hillslope orientation, and land cover, all of which are known to affect the distribution of frozen ground (Fox, 1992; MacKinney, 1929; Wilcox et al., 1997; Willis et al., 1961).
- 4.) The modCFGF model produces more accurate frost depths than the CFGF for all ~~but one of the~~ six test sites in the W-3 watershed. Overall, the modCFGF model more accurately captures the inter-annual variability in frost depth at a given site and variability of frost depth between sites. Although both the CFGF and modCFGF capture the majority of frozen ground events observed, the modCFGF model has ~~42.5~~ 15.2% better accuracy in capturing the presence of frozen ground, which is expected to be important for capturing runoff that is produced by frozen ground.
- 5.) A key reason for the difference in performance between the two frost models is that the modCFGF model includes the insulation of the ground by ground cover while the CFGF model does not. When ground cover is removed from the modCFGF model, its results for W-3 are less accurate and the variability in simulated frost depth between the

sites is limited. Ground cover is likely important in this watershed because it is relatively thick and is also present at all stages of the winter while snowpack is not.

Formatted: Indent: First line: 0.5"

~~Four~~Overall, the modCFGI model provides improved spatial representation of frozen ground while requiring only cloud cover estimates as additional forcing data (more forcing data may be required if soil moisture is simulated to obtain frost depth). Limited data requirements should make modCFGI well-suited for data sparse environments. Hydrologic models often need to account for the presence of frozen ground, which in data-sparse environments often means using simple degree-day approaches that typically vary frozen ground with elevation only (as was shown with the CFGI model). To calculate  $T_{rad}$  the modCFGI model does require cloud cover data, which are collected operationally at most airports within the U.S. If soil moisture is explicitly simulated within the hydrologic model the modCFGI model can also be used with the modified Berggren Equation to simulate frost depth, which requires information on soil type and an estimate of the thermal conductivity of the soil.

Five main avenues are available for future research. First, the modCFGI model should be generalized to include the effects of wind (as it relates to the snowpack) and more completely consider the role of soil moisture. Soil moisture is not considered when calculating the frost index, so it does not impact the initiation or duration of frozen ground. This limitation results from using a degree-day approach and may be important in some cases (Kurganova et al., 2007; Willis et al., 1961). Second, the modCFGI model should be tested further. Additional testing should consider other areas where snow and frozen ground are known to affect runoff, such as the Upper Midwest region of the United States. Additional testing should also better characterize the insulation properties of ground cover under different management scenarios. ~~Third~~Third, the calculation of  $T_{rad}$  is simple and applicable in data-sparse environments, but other approaches for adjusting a temperature value based on topography and land cover are available (Fox, 1992; Kang, 2005; Webster et al., 2017) and could be further tested. Fourth, future research should also determine the effects of spatial heterogeneity of snow and frost depth on runoff and streamflow at both the local and watershed scales. Similar to Campbell et al. (2010), the RTI and modCFGI models could be used in data-sparse watersheds to investigate how changes in historic and future climate affect snow, frozen ground, and runoff. Finally, although this paper focuses on the simulation of frost depth in the context of watershed modelling, the methods described could also be used for agriculture, overland mobility modelling, and infrastructure where snow and frost depth are major concerns.

## References

- Aldrich Jr, H.P.: Frost penetration below highway and airfield pavements, Highway Research Board Bulletin (135), 124, 1956.
- Allen, R.G., Walter, I.A., Elliott, R., Howell, T., Itenfisu, D., Jensen, M.: The ASCE Standardized Reference Evapotranspiration Equation, ASCE, 2005.

- ~~Anderson, E., Greenan, H., Wipkey, R., Machell, C.: Watershed Hydro Climatology and Data for Water Years 1960-1974, NOAA ARS Cooperative Research Project, US Dept. of Commerce and US Dept. of Agriculture, 1974.~~
- Anderson, E.A.: National Weather Service River Forecast System - Snow Accumulation and Ablation Model, Technical Memorandum NWS Hydro-17, November 1973, 217 pp., Silver Spring, Maryland, 1973.
- 5 Anderson, E.A.: A Point Energy and Mass Balance Model of a Snow Cover, U.S. National Oceanic and Atmospheric Administration NOAA Technical Report NWS 9, Silver Spring, Maryland, 1976.
- Anderson, E.A.: Snow Accumulation and Ablation Model - SNOW-17, NWSRFS User Documentation, U.S. National Weather Service, Silver Springs, MD, 2006.
- Aquaveo: Watershed Modeling System Version 9.1.4, Provo, Utah, 2013.
- 10 Bayard, D., Stähli, M., Parriaux, A., Flüeler, H.: The influence of seasonally frozen soil on the snowmelt runoff at two Alpine sites in southern Switzerland, Journal of Hydrology 309(1), 66-84, 2005.
- Beck, P.S., Atzberger, C., Høgda, K.A., Johansen, B., Skidmore, A.K.: Improved monitoring of vegetation dynamics at very high latitudes: A new method using MODIS NDVI, Remote Sensing of Environment, 100(3), 321-334, 2006.
- Bras, R.L.: Hydrology: An Introduction to Hydrologic Science, Addison-Wesley, Reading, Massachusetts, 643 pp., 1990.
- 15 Brown, J.: Influence of vegetation on permafrost, In: Woods, K.B. (Ed.), Permafrost International Conference, National Academy of Sciences-National Research Council, NRC Div. Bldg., Ottawa, Canada, 6 pp., 1966.
- Campbell, J.L., Ollinger, S.V., Flerchinger, G.N., Wicklein, H., Hayhoe, K., Bailey, A.S.: Past and projected future changes in snowpack and soil frost at the Hubbard Brook Experiment Forest, New Hampshire, USA, Hydrological Processes, 24, 2465-2480, 2010.
- 20 Carey, S.K., Woo, M.-k.: Freezing of subarctic hillslopes, Wolf Creek Basin, Yukon, Canada. Arctic, Antarctic, and Alpine Research, 37(1), 1-10, 2005.
- Chen, R.S., Kang, E.S., Ji, X.B., Yang, Y., Zhang, Z.H., Qing, W.W., Bai, S.Y., Wang, L.D., Kong, Q.Z., Lei, Y.H., Pei, Z.X.: Preliminary study of the hydrological processes in the alpine meadow and permafrost regions at the headwaters of Heihe River, Journal of Glaciology and Geocryology, 29(3), 387-396, 2007.
- 25 De Roo, A., Odijk, M., Schmuck, G., Koster, E., Lucieer, A.: Assessing the effects of land use changes on floods in the Meuse and Oder catchment, Physics and Chemistry of the Earth, Part B: Hydrology, Oceans and Atmosphere, 26(7), 593-599, 2001.
- DeWalle, D.R., Rango, A.: Principles of Snow Hydrology, Cambridge University Press, 2008.
- Diebold, C.H.: The effects of vegetation upon snow cover and frost penetration during the March 1936 floods, Journal of Forestry, 36(11), 1131-1137, 1938.
- 30 Doherty, J., Brebber, L., Whyte, P.: PEST: Model-Independent Parameter Estimation, Watermark Computing, Corinda, Australia, 122, Journal of Forestry, 36, 1131-1137, 1994.
- Downer, C.W., Ogden, F.L.: GSSHA: Model to simulate diverse stream flow producing processes, Journal of Hydrologic Engineering, 9(3), 161-174, 2004.

- Downer, C.W., Ogden, F.L.: GSSHA Users' Manual. In: SR-06-1, E.C. (Ed.), U.S. Army Engineer Research and Development Center, Vicksburg, Mississippi, 2006.
- Downer, C.W.: Development of a Simple Soil Moisture Model in the Hydrologic Simulator GSSHA, ERDC-TN-SWWRP-07-8, U.S. Army Engineer Research and Development Center, Vicksburg, Mississippi, 2007.
- 5 Duffie, J.A., Beckman, W.A.: Solar Engineering of Thermal Processes, 3, Wiley, New York, 1980.
- Dun, S., Wu, J., McCool, D., Frankenberger, J., Flanagan, D.: Improving frost-simulation subroutines of the Water Erosion Prediction Project (WEPP) model, Transactions of the ASABE, 53(5), 1399-1411, 2010.
- Dunne, T., Black, R.D.: An experimental investigation of runoff production in permeable soils, Water Resources Research, 6(2), 478-490, 1970a.
- 10 Dunne, T., Black, R.D.: Partial area contributions to storm runoff in a small New England watershed, Water Resources Research, 6(5), 1296-1311, 1970b.
- Dunne, T., Black, R.D.: Runoff processes during snowmelt, Water Resources Research, 7(5), 1160-1172, 1971.
- Fahey, T.J., Lang, G.E.: Concrete frost along an elevational gradient in New Hampshire, Canadian Journal of Forest Research, 5(4), 700-705, 1975.
- 15 Farouki, O.T.: The thermal properties of soils in cold regions, Cold Regions Science and Technology, 5(1), 67-75, 1981.
- Fassnacht, S.R., López-Moreno, J.I., Ma, C., Weber, A.N., Pfohl, A.K.D., Kampf, S.K., Kappas, M.: Spatio-temporal snowmelt variability across the headwaters of the Southern Rocky Mountains, Frontiers of Earth Science, 1-10, 2017.
- Flerchinger, G., Saxton, K.E.: Simultaneous heat and water model of a freezing snow-residue-soil system I, Theory and development, Transactions of the ASAE, 32(2), 565-0571, 1989.
- 20 Follum, M.L., Downer, C.W., Niemann, J.D.: Simulating the spatial distribution of snow pack and snow melt runoff with different snow melt algorithms in a physics based watershed model, AGU Fall Meeting, American Geophysical Union, San Francisco, CA, 2014.
- Follum, M.L., Downer, C.W., Niemann, J.D., Roylance, S.M., Vuyovich, C.M.: A radiation-derived temperature-index snow routine for the GSSHA hydrologic model, Journal of Hydrology, 529, Part 3, 723-736, 2015.
- 25 Fox, J.D.: Incorporating freeze-thaw calculations into a water balance model, Water Resources Research, 28(9), 2229-2244, 1992.
- Fry, J.A., Xian, G., Jin, S., Dewitz, J.A., Homer, C.G., Limin, Y., Barnews, C.A., Helold, N.D., Wickham, J.D.: Completion of the 2006 national land cover database for the conterminous United States, Photogrammetric Engineering and Remote Sensing, 77(9), 858-864, 2011.
- 30 Gesch, D., Oimoen, M., Greenlee, S., Nelson, C., Steuck, M., Tyler, D.: The national elevation dataset, Photogrammetric Engineering and Remote Sensing, 68(1), 5-32, 2002.
- Green, W., Ampt, G.: Studies on Soil Physics, The Journal of Agricultural Science, 4(01), 1-24, 1911.

- ~~Hedstrom, N.R., Pomeroy, J.W.: Measurements and modelling of snow interception in the boreal forest, *Hydrological Processes*, 12(10-11), 1611-1625, 1998.~~
- ~~Gustafson, J.R., Brooks, P.D., Molotch, N.P., Veatch, W.C.: Estimating snow sublimation using natural chemical and isotropic tracers across a gradient of solar radiation, *Water Resources Research*, 46(12), 1-14, 2010.~~
- 5 

Henneman, H.E., Stefan, H.G.: Albedo models for snow and ice on a freshwater lake, *Cold Regions Science and Technology*, 29(1), 31-48, 1999.
- ~~Jansson, P.E.: Coupled heat and mass transfer model for soil-plant-atmosphere systems. 2001.~~
- ~~Jansson, P.E., Karlberg, L.: Coupled heat and mass transfer model for soil-plant-atmosphere systems, *Royal Institute of Technology, Stockholm*, p. 454, 2010.~~
- 10 

Johansen, O.: Thermal Conductivity of Soils, CRREL-TL-637, Cold Regions Research and Engineering Laboratory, Hanover, NH, 1977.
- ~~Johnson, C.W., McArthur, R.P.: Winter storm and flood analyses, northwest interior, *Hydraulic Engineering and the Environment, ASCE*, 359-369, 1973.~~
- Jost, G., Weiler, M., Gluns, D.R., Alila, Y.: The influence of forest and topography on snow accumulation and melt at the watershed-scale, *Journal of Hydrology*, 347(1), 101-115, 2007.
- 15 

~~Kang, D.H.: Distributed Snowmelt Modeling with GIS and CASC2D at California Gulch, Colorado, Colorado State University, Fort Collins, CO, p. 195, 2005.~~
- Kennedy, I., Sharratt, B.: Model Comparisons to Simulate Soil Frost Depthwi, *Soil Science*, 163(8), 636-645, 1998.
- Koren, V., Schaake, J., Mitchell, K., Duan, Q.Y., Chen, F., Baker, J.M.: A parameterization of snowpack and frozen ground intended for NCEP weather and climate models, *Journal of Geophysical Research: Atmospheres* (1984–2012), 104(D16), 19569-19585, 1999.
- 20 

Kurganova, I., Teepe, R., Loftfield, N.: Influence of freeze-thaw events on carbon dioxide emission from soils at different moisture and land use, *Carbon Balance and Management*, 2, 2-2, 2007.
- Lin, C., McCool, D.: Simulating snowmelt and soil frost depth by an energy budget approach, *Transactions of the ASABE*, 49(5), 1383-1394, 2006.
- 25 

~~Lindstrom, G., Bishop, K., Lofvenius, M.O.: Soil frost and runoff at Svartberget, northern Sweden—Measurements and model analysis, *Hydrological Processes*, 16, 3379–3392, 2002.~~
- Liou, K.N.: An Introduction to Atmospheric Radiation, second edition, Academic Press, New York, 2002.
- Liston, G.E., Elder, K.: A distributed snow-evolution modeling system (SnowModel), *Journal of Hydrometeorology*, 7(6), 1259-1276, 2006.
- 30 

MacKinney, A.: Effects of forest litter on soil temperature and soil freezing in autumn and winter, *Ecology*, 10(3), 312-321, 1929.
- ~~McNamara, J.P., Kane, D.P., Hinzman, L.D.: Hydrograph separation in an Arctic watershed using mizing model and graphical techniques, *Water Resources Research*, 33, 1707-1719, 1997.~~

Molnau, M., Bissell, V.C.: A continuous frozen ground index for flood forecasting, Proceedings 51st Annual Meeting Western Snow Conference, Canadian Water Resources Association, Cambridge, Ontario, 109-119, 1983.

Monteith, J.: Evaporation and environment, Symposia of the Society for Experimental Biology, 4, 1965.

Monteith, J.: Evaporation and surface temperature, Quarterly Journal of the Royal Meteorological Society, 107(451), 1-27, 1981.

Musselman, K., Molotch, N.P., Brooks, P.D.: Effects of vegetation on snow accumulation and ablation in a mid-latitude sub-alpine forest, Hydrological Processes, 22(15), 2767-2776, 2008.

Nikolaev, I.V., Leong, W.H., Rosen, M.A.: Experimental investigation of soil thermal conductivity over a wide temperature range, International Journal of Thermophysics, 34(6), 1110-1129, 2013. ▲

Nyberg, L., Stähli, M., Mellander, P.E., Bishop, K.: Soil frost effects on soil water and runoff dynamics along a boreal forest transect: 1. Field investigations, Hydrological Processes, 15, 909 – 926, 2001.

Ogden, F.L., Saghaian, B.: Green and Ampt infiltration with redistribution, Journal of Irrigation and Drainage Engineering, 123(5), 386-393, 1997.

Pearson, G.A.: Factors controlling the distribution of forest types, Part I, Ecology, 1(3), 139-159, 1920.

Pomeroy, J.: Wind Transport of Snow, PhD Thesis, University of Saskatchewan, 1988.

Pomeroy, J., Gray, D., Hedstrom, N., Janowicz, J.: Prediction of seasonal snow accumulation in cold climate forests, Hydrological Processes, 16(18), 3543-3558, 2002.

~~Pomeroy, J., Parviainen, J., Hedstrom, N., Gray, D.: Coupled modelling of forest snow interception and sublimation, Hydrological processes, 12(15), 2317-2337, 1998.~~

~~Pomeroy, J., Schmidt, R.: The use of fractal geometry in modeling intercepted snow accumulation and sublimation, Proceedings of the Eastern Snow Conference, 1-10, 1993.~~

Prévost, M., Barry, R., Stein, J., Plamondon, A.P.: Snowmelt runoff modelling in a balsam fir forest with variable source are simulator (VSAS2), Water Resources Research, 25(5), 1067-1077, 1990.

Rawls, W., Brakensiek, D., Saxton, K.: Estimation of soil water properties, Transactions of the ASAE, 25(5), 1316-1320, 1982.

Rawls, W.J., Brakensiek, D.: Prediction of soil water properties for hydrologic modelling, In: Watershed Management in the Eighties, ASCE, 293-299, 1985.

Rawls, W.J., Brakensiek, D.L., Miller, N.: Green-Ampt infiltration parameters from soils data, Journal of Hydraulic Engineering, 109(1), 62-70, 1983.

Rekolainen, S., Posch, M.: Adapting the CREAMS model for Finnish conditions, Hydrology Research, 24(5), 309-322, 1993.

Ricard, J.A., Tobiasson, W., Groatorex, A.: The field assembled frost gage, United States Army Cold Regions Research and Engineering Laboratory, Hanover, New Hampshire, 1976.

Formatted: Font: Times New Roman, English (U.S.)

[Rinehart, A.J., Vivoni, E.R., Brooks, P.D.: Effects of vegetation, albedo, and solar radiation sheltering on the distribution of snow in the Valles Caldera, New Mexico, Ecohydrology, 1\(3\), 253-270, 2008.](#)

Sartz, R.S.: Effect of Forest Cover Removal on Depth of Soil Freezing and Overland Flow, Soil Science Society of America Journal, 37(5), 774-777, 1973.

5 Shanley, J.B.: Sleepers River, Vermont: A water, energy, and biogeochemical budgets program site, Fact Sheet-166-99, U.S. Department of the Interior, U.S. Geological Survey, 2000.

Shanley, J.B., Chalmers, A.: The effect of frozen soil on snowmelt runoff at Sleepers River, Vermont, Hydrological Processes, 13(13), 1843-1857, 1999.

10 Shanley, J.B., Sundquist, E.T., Kendall, C.: Water, energy, and biogeochemical budget research at Sleepers River Research Watershed, Vermont, 2331-1258, U.S. Geological Survey, Open-File Reports Section [distributor], 1995.

Sicart, J.E., Pomeroy, J.W., Essery, R.L.H., Hardy, J., Link, T., Marks, D.: A sensitivity study of daytime net radiation during snowmelt to forest canopy and atmospheric conditions, Journal of Hydrometeorology, 5(5), 774-784, 2004.

Smith, J.A.: Precipitation. In: Maidment, D.R. (Ed.), Handbook of Hydrology, McGraw-Hill Inc., New York, 3.4, 1993.

15 ~~Stoner, J.D., Lorenz, D.L., Wiehe, G.J., Goldstein, R.M.: Red River of the North Basin, Minnesota, North Dakota, and South Dakota, Journal of the American Water Resources Association, 29(4), 575-615, 1993.~~

[Stähli, M., Jansson, P-E., Lundin, L-C.: Soil moisture redistribution and infiltration in frozen sandy soils, Water Resources Research 35\(1\), 95-103, 1999.](#)

[Stähli, M.: Hydrological significance of soil frost for pre-alpine areas, Journal of Hydrology, 546, 90-102, 2017.](#)

20 TVA.: Heat and Mass Transfer Between a Water Surface and the Atmosphere, Tennessee Valley Authority, Norris, TN, 1972.

Van Der Knijff, J., Younis, J., De Roo, A.: LISFLOOD: a GIS-based distributed model for river basin scale water balance and flood simulation, International Journal of Geographical Information Science, 24(2), 189-212, 2010.

[Veatch, W., Brooks, P.D., Gustafson, J.R., Molotch, N.P.: Quantifying the effects of forest canopy cover on net snow accumulation at a continental, mid-latitude site, Ecohydrology, 2\(2\), 115-128, 2009.](#)

25 Vermette, S., Christopher, S.: Using the rate of accumulated freezing and thawing degree days as a surrogate for determining freezing depth in a temperate forest soil, Middle States Geographer, 41, 68-73, 2008.

Vermette, S., Kanack, J.: Modeling frost line soil penetration using freezing degree-day rates, day length, and sun angle, 69th Eastern Snow Conference, Frost Valley YMCA, Claryville, New York, USA, 2012.

30 Wang, Q., Adiku, S., Tenhunen, J., Granier, A.: On the relationship of NDVI with leaf area index in a deciduous forest site, Remote Sensing of Environment, 94(2), 244-255, 2005.

[Webster, C., Rutter, N., Jonas, T.: Improving representation of canopy temperatures for modeling subcanopy incoming longwave radiation to the snow surface, Journal of Geophysical Research: Atmospheres 122\(17\), 9154-9172, 2017.](#)

Wilcox, B.P., Newman, B.D., Brandes, D., Davenport, D.W., Reid, K.: Runoff from a semiarid ponderosa pine hillslope in New Mexico. Water Resources Research, 33(10), 2301-2314, 1997.

Willis, W., Carlson, C., Alessi, J., Haas, H.: Depth of freezing and spring run-off as related to fall soil-moisture level, Canadian Journal of Soil Science, 41(1), 115-123, 1961.

Woo, M., Arain, M., Mollinga, M., Yi, S.: A two-directional freeze and thaw algorithm for hydrologic and land surface modelling, Geophysical Research Letters, 31(12), 2004.

5 | Woo, M.: Permafrost hydrology in North America, Atmosphere-Ocean, 24(3), 201-234, 1986.

**Formatted:** Font: Times New Roman